

Thermomechanical Characterization of Variable Force NiTi Orthodontic Archwires

Anjali Sudershan Krishan Mehta
Marquette University

Recommended Citation

Mehta, Anjali Sudershan Krishan, "Thermomechanical Characterization of Variable Force NiTi Orthodontic Archwires" (2015).
Master's Theses (2009 -). Paper 328.
http://epublications.marquette.edu/theses_open/328

**THERMOMECHANICAL CHARACTERIZATION OF
VARIABLE FORCE NITI ORTHODONTIC
ARCHWIRES**

by

Anjali Mehta, BDS MDS

A Thesis Submitted to the Faculty of the Graduate School,
Marquette University,
in Partial Fulfillment of the Requirements for
the Degree of Master of Science

Milwaukee, Wisconsin

August 2015

ABSTRACT
THERMOMECHANICAL CHARACTERIZATION OF VARIABLE
FORCE NITI ORTHODONTIC ARCHWIRES

Anjali Mehta, BDS MDS

Marquette University, 2015

Introduction: Nickel-Titanium (NiTi) archwires, due to their properties of superelasticity and shape memory, have been extensively used in orthodontic mechanotherapy. However, one of the shortcomings of these wires is that they deliver constant forces across the entire arch. The amount of force needed to move a tooth is a function of the surface area of the tooth and its supporting bone; and is lesser for single rooted anterior teeth compared to larger molars. The introduction of heat treatment of NiTi wires and the influence of varying temperature and duration of heat treatment on the transition temperature range has provided wires with variable forces across different sections of the same archwire.

Objectives: This study investigated the thermal behavior and load-deflection characteristics of different brands of variable force archwires across sections of the archwire.

Materials and Method: Five brands of variable force orthodontic wires of 0.016 X 0.016 inch were compared against a non-variable force brand to evaluate their thermomechanical characteristics using Differential Scanning Calorimetry (DSC) and a three point bending test. Three segments (anterior, premolar and molar) of each type of wire were evaluated and compared. Two-way ANOVA was used to statistically analyze the thermal and bending measures.

Results: The anterior segments of the variable force orthodontic wires exhibited significantly ($p < 0.05$) greater austenite finish temperatures and lower loads compared to the molar segments. Significant ($p < 0.05$) differences in thermal and bending values were observed between different brands of variable force wires and the control.

Conclusion: Marketed variable force orthodontic wires do in fact deliver different force values depending on region (anterior, premolar, molar) and do so as a result of manufacturing steps that alter their thermal transitions. Differences exist among brands suggesting they are not interchangeable.

ACKNOWLEDGEMENTS

Anjali Mehta, BDS MDS

I would like to thank my program director Dr. David Berzins for all the help and support in finding my topic of research and serving as my thesis director and mentor throughout this project. In addition, I would also like to thank my research committee, Dr. T. Gerard Bradley, Dr. Jeffrey Toth, and Dr. Howard Roberts for their help and participation in this project.

I would like to thank Dr. Naveen Bansal for his statistical guidance and support in this project.

TABLE OF CONTENTS

ACKNOWLEDGEMENTS.....	i
LIST OF TABLES	iii
LIST OF FIGURES	iv
CHAPTER	
I. INTRODUCTION	1
II. LITERATURE REVIEW.....	3
III. MATERIALS AND METHODS.....	14
IV. RESULTS	18
V. DISCUSSION.....	41
VI. CONCLUSIONS.....	47
REFERENCES	48

LIST OF TABLES

Table 1.	Brand names and manufacturers of wires of different groups	14
Table 2.	DSC measured Austenitic temperatures and enthalpy changes for phase transformations in the heating within three segments for all six groups of wires	24
Table 3.	Comparison of DSC measured Austenitic temperatures and enthalpy changes for phase transformation during heating within the three segments for five brands of variable force wires	25
Table 4.	DSC measured R phase and martensitic temperatures, and enthalpy for phase transformation during cooling in the six groups	26
Table 5.	Comparison of DSC measured R phase and Martensitic temperatures, and enthalpy changes for phase transformation during cooling within the three segments for five brands of variable force wires	27
Table 6.	Elastic modulus, stiffness and load at 1 mm, 2 mm and 3 mm deflection curves during activation	34
Table 7.	Elastic modulus, stiffness and load at 1 mm, 2 mm and 3 mm deflection curves during deactivation	35
Table 8.	Comparison between Variable Force Wire Brands within different segments during activation	36
Table 9.	Comparison between Variable Force Wire Brands within different segments during deactivation	37

LIST OF FIGURES

Figure 1.	Illustration showing 4 mm segment samples as taken from the anterior, premolar and molar segments from the archwires for the DSC test	15
Figure 2.	DSC heating and cooling curves of Anterior, Premolar and Molar segments of BioForce orthodontic wires	19
Figure 3.	DSC heating and cooling curves of Anterior, Premolar and Molar segments of IonGuard BioForce orthodontic wires	19
Figure 4.	DSC heating and cooling curves of Anterior, Premolar and Molar segments of TriTanium orthodontic wires	20
Figure 5.	DSC heating and cooling curves of Anterior, Premolar and Molar segments of Titanol Triple Force orthodontic wires	20
Figure 6.	DSC heating and cooling curves of Anterior, Premolar and Molar segments of Tri-Force Thermal orthodontic wires	21
Figure 7.	DSC heating and cooling curves of Anterior, Premolar and Molar segments of NeoSentalloy orthodontic wires	21
Figure 8.	DSC heating and cooling curves of Anterior segments of six groups of wires	22
Figure 9.	DSC heating and cooling curves of Premolar segments of six groups of wires	22
Figure 10.	DSC heating and cooling curves of Molar segments of six groups of wires	23
Figure 11.	Force deflection curves for Anterior, Premolar and Molar segments of BioForce wires	28
Figure 12.	Force deflection curves for Anterior, Premolar and Molar segments of IonGuard BioForce wires	29
Figure 13.	Force deflection curves for Anterior, Premolar and Molar segments of TriTanium wires	29
Figure 14.	Force deflection curves for Anterior, Premolar and Molar segments of Titanol Triple Force wires	30

Figure 15.	Force deflection curves for Anterior, Premolar and Molar segments of Tri-Force Thermal wires	30
Figure 16.	Force deflection curves for Anterior, Premolar and Molar segments of NeoSentalloy wires	31
Figure 17.	Force deflection curves for Anterior segment of six brands of wires	31
Figure 18.	Force deflection curves of Premolar segment of six brands of wires	32
Figure 19.	Force deflection curves for Molar segments of six brands of wires	32
Figure 20.	Graph comparing mean A_f temperatures of Anterior, Premolar and Molar segments with deactivation forces at 2 mm for BioForce archwires	38
Figure 21	Graph comparing mean A_f temperatures of Anterior, Premolar and Molar segments with bending forces at 2 mm deactivation for BioForce IonGuard archwires	38
Figure 22.	Graph comparing mean A_f temperatures of Anterior, Premolar and Molar segments with deactivation forces at 2 mm for TriTanium archwires	39
Figure 23.	Graph comparing mean A_f temperatures of Anterior, Premolar and Molar segments with deactivation forces at 2 mm for Titanol Triple Force archwires	39
Figure 24.	Graph comparing mean A_f temperatures of Anterior, Premolar and Molar segments with deactivation forces at 2 mm for Tri-Force Thermal archwires	40
Figure 25.	Graph comparing mean A_f temperatures of Anterior, Premolar and Molar segments with deactivation forces at 2 mm for NeoSentalloy archwires	40

CHAPTER 1

INTRODUCTION

Fixed appliance mechanotherapy involves the correction of malocclusions through the application of light and continuous forces, which can produce optimal tooth movement through the remodeling of the surrounding bone and periodontal tissues. (Proffit et al., 2013). These forces are delivered to the tooth and its supporting structures through the stored energy within the activated appliance system, of which one of the major components is the orthodontic archwire.

Nickel-Titanium (NiTi) archwires, due to their properties of superelasticity and shape memory, have been extensively used in orthodontic mechanotherapy (Iijima et al., 2002). These wires are characterized by a wide elastic range or high springback and flexibility (Khier et al., 1991). An important metallurgical feature of these wires is that they have a wide load-deflection range and remain activated over a prolonged period of time, delivering near constant stresses during deactivation, thus making them suitable for orthodontic tooth movement (Miura et al., 1986). This is due to their phase transformation behavior under the influence of stresses at body temperature, which allows for fairly large amounts of deflection of the archwires without permanent deformation (Nikolai, 1997). Thus, they are especially useful in the initial alignment of teeth (Andreasen & Barrett, 1973; Proffit et al., 2013).

NiTi superelastic behavior can be influenced by its chemical composition and manufacturing processes such as cold working and heat treatment (Pelton et al., 2000). Heat treatment has been shown to influence both transition temperatures and the stress

levels (loads) at which these wires undergo phase transformation (Khier et al., 1991). The amount of orthodontic force produced is a function of the amount of force applied by the archwire and the root surface area of the tooth to be moved and its supporting bone; and should be lesser for the single rooted anterior teeth as compared to the larger molars (Santoro et al., 2001). One of the disadvantages of NiTi archwires is that they deliver a constant force across the arch (Gil et al., 2013). The introduction of heat treatment of superelastic NiTi wires and the influence of varying temperature and duration of heat treatment on transition temperature range has led to the development of wires with variable force across different sections in the same archwire (Miura et al., 1986; Miura, 1991). These wires offer the advantage of optimizing the amount of force delivered in the different segments of the arch and thus render it possible to use rectangular superelastic archwires in the initial stages of fixed appliance thereby reducing the number of wires used and thus reducing treatment times (Ibe & Segner, 1998). Various brands of variable force archwires are available. However, there is not enough research to support the claims made by the manufacturers that the force levels are variable between the segments. Hence, the present study aimed at investigating variable force archwires and evaluating their thermal behavior and load-deflection characteristics across the sections of the archwires.

CHAPTER 2

LITERATURE REVIEW

Application of light, continuous forces has been considered an important feature in achieving sustained tooth movement and reducing patient discomfort (Kusy, 1997; Proffit et al., 2013). Orthodontic treatment mechanics is based on the utilization of energy stored within an appliance system that has been activated to achieve tooth movement (Quintao & Brunharo, 2009). Orthodontic archwires form an integral part of this appliance system and play an important role in optimizing the amount of load distributed to the teeth and their surrounding periodontal tissues. Towards achieving this goal, desirable characteristics of an ideal archwire system include low stiffness, flexibility, high springback, formability, high energy storage capacity, esthetics, biocompatibility, low surface friction and welding or soldering capability (Kapila & Sachdeva, 1989; Kusy, 1997; Brantley & Eliades, 2001). Over the years, the materials used for fabrication of orthodontic archwires have undergone dramatic improvement beginning from Angle's era when gold wires, made of Type IV gold, were considered the "gold standard" (Nickolai, 1997; Brantley & Eliades, 2001). Today, wires are fabricated mainly from four types of alloy systems, viz. stainless steel, cobalt-chromium, nickel-titanium and beta-titanium (Kusy, 1997).

Nickel-Titanium Wires In Orthodontics

Nickel-Titanium wires have been successfully used during various stages of fixed appliance treatment due to the various advantages they offer, such as superelasticity, low

load deflection and shape memory. Force levels delivered by these wires can be influenced by modifying their composition or heat treatment of these wires during manufacture, making it possible to use different force levels without having to change the diameter of the archwire (Miura et al., 1986), and the use of rectangular wires in early stages of treatment (Miura, 1991). This allows for early engagement of brackets and thus, controlled tooth movement early during orthodontic mechanotherapy which in turn results in a reduced number of wire changes during treatment, thus reducing treatment times. The near constant force levels during deactivation over a wide range by these wires allows for longer intervals between patient visits and reduces patient discomfort due to the near-physiologic forces imparted to the periodontal tissues. Thus, the use of NiTi allows for improved patient outcomes and a reduction in chairside time and clinical armamentarium (Andreasen & Barrett, 1973; Andreasen & Morrow, 1978). Hence, these archwires are commonly used in fixed appliance mechanotherapy. However, some of the disadvantages of NiTi wires are increased roughness which increases with clinical use, thus increasing friction, no formability, and uniform force levels distributed across the archwire. In addition, it is difficult, if not impossible, to solder or weld them (Andreasen & Morrow, 1978; Kusy, 1997; Gil et al., 2013).

History & Evolution of Nickel-Titanium Archwires

Nickel-Titanium alloy or nitinol was first developed by Buehler in 1962 at the U.S. Naval Ordnance Laboratory in White Oak, Maryland. This alloy is an intermetallic compound with a near equiatomic ratio of nickel and titanium. The name was an acronym derived from its composition of nickel and titanium, and the Naval Ordnance Lab, where

it was first developed (Andreasen & Barrett, 1973). Nickel-Titanium may exhibit shape memory and superelasticity that have been attributed to a reversible and diffusion-less solid-state phase transformation of the alloy. The phase transformation takes place between a higher temperature austenite phase and a lower temperature martensite phase (Thompson 2000). The austenite phase is a body centered cubic crystal structure while the atomic lattice of the martensitic phase has been described as monoclinic, triclinic or closed packed hexagonal crystal structure (Brantley & Eliades, 2001). When the alloy is heated, the temperature at which the martensitic phase begins to transform to austenite is referred to as the austenitic start (A_s) temperature, and the temperature at which the alloy is completely transformed to austenite is the austenitic finish temperature (A_f). Similarly, when the alloy is cooled from its austenitic phase to martensite, the initiation of phase conversion to martensite is referred to as the martensite start (M_s) temperature and complete transformation to the martensite phase is the martensitic finish (M_f) temperature. The martensitic phase of nickel-titanium is more ductile and is associated with a lower elastic modulus and electrical resistivity as compared to the austenitic phase (Thompson, 2000) and can be modified in shape during this phase. When the alloy is reheated to a temperature above its transition temperature, it regains its original shape, a property which is referred to as the “shape memory effect” and this alloy has been referred to as a smart material. Similarly, this transition from austenitic to martensitic phase can also be induced by the application of force or stress, a phenomenon which is referred to as a stress-induced martensitic transformation (SIM), and accounts for the superelasticity or pseudo-elasticity of this alloy (Kusy, 1997; Thompson, 2000).

The development of nickel-titanium had huge ramifications in the medical and dental world and led to the introduction of nickel-titanium in the specialty of orthodontics as an archwire material by Andreasen and others in 1971 (Andreasen & Barrett, 1973). The first nickel-titanium wires were marketed as Nitinol by Unitek Corporation (Kusy, 1997). These wires were characterized by low stiffness, a low elastic modulus and high springback, but did not demonstrate the shape memory effect in the temperature range at which they were used and were in their martensitic phase and thus martensite stabilized archwires (Kusy, 1997).

Ongoing research led to the development of the second generation superelastic or pseudoelastic NiTi alloys in the 1980s (Burstone et al., 1985; Miura et al., 1986; Kusy 1997). These wires, referred to as Chinese NiTi and Japanese NiTi were characterized by flexibility and nonlinear stress versus strain behavior with near constant stress/force produced over a wide range of deflection during deactivation when the wires are in their martensitic phase. This superelastic or pseudoelastic behavior of these nickel-titanium archwires has been attributed to the stress-induced phase transformation of these wires from austenite to martensite. These wires are typically in their austenitic phase at room temperature and when the wire is loaded or unloaded it is this phase transformation and the associated metallurgical change of the crystal structure from body centered cubic to closed pack hexagonal martensite which accounts for the horizontal plateauing of the stresses generated in the loading and unloading of the wire. This phase transformation begins at about 2% change in strain application of the wire to about 8-10% and the wire resists permanent deformation due to this phase transformation (Miura et al., 1986). This

phase change is responsible for the constant levels of forces delivered by these wires during prolonged periods of activation and deactivation.

Heat treatment of the Japanese nickel-titanium wires by two different modes were proposed by Miura et al. (1986, 1988). They investigated the effects of heat treatment on the mechanical behavior of the Japanese nickel-titanium wires, which were heated in an immersion nitrate salt bath for varying periods of time and at different temperatures, followed by quenching in water. Heat treatment at 500°C for a period of 2 hours resulted in a reduction in the superelastic load levels delivered by the wire as compared to untreated wires. However, an increase in the heat treatment temperature to 600°C even for 5 minutes resulted in loss of springback and superelastic properties of the archwire. They concluded that heat treatment of nickel-titanium wires could be used as a method to individualize the amount of force delivered by a wire without changing its dimension or bending any loops in the wire. They also introduced the concept of individualized force levels being delivered in different segments of the same archwire by controlled heat treatment on different sections of the wire. With this, the application of controlled heat with adequate temperature and time on the anterior segment of the archwire could be used to reduce the amount of force within the anterior segment while not disturbing the posterior segment of the archwire.

In a continuation of their research on the influence of heat treatment on the Japanese NiTi wire, Miura et al. heat treated these wires using the direct electric resistance heat treatment (DERHT) method by applying electric current for varying amounts of time in different regions of the wire. An application of 3.5 A of current for 60 minutes in the anterior segment and 15 minutes in the premolar region resulted in

progressively increasing load levels to produce a superelastic plateau in the wire. The superelastic plateau observed in the anterior region was as low as 80 gm. The application of current did not affect the springback property of the wire and offered the advantages of the apparatus being light weight and not bulky. Also, with the use of electric pliers it was possible to localize the area of heat application to a small region.

This research led to the marketing of the third generation of nickel-titanium archwires which were thermo-responsive and exhibited true shape memory. Nickel-Titanium wires developed in the 1990s by GAC International (NeoSentalloy) (Brantley & Eliades, 2001) belonged to this group. Typically, these wires have a transition temperature in the same range as body temperature and hence exhibit the shape memory effect when placed in the oral cavity (Brantley & Eliades, 2001). Below the austenitic-start temperature these wires exist in their more ductile, martensitic form and can be relatively easily deformed or adapted to malpositioned or crowded teeth. On reaching their austenitic finish temperature, once placed in the oral cavity, these archwires transform to their austenitic phase, thus exhibiting their shape memory and revert back to their original shape. Also included in this group were the CuNiTi archwires, which are available in A_f transition temperatures of 35°C and 40°C. Santoro et al. (2001) and Kusy (1997) reported that the CuNiTi wires of different transition temperatures are a result of varying the amount of copper and chromium in their composition. However, a SEM/EDS evaluation study has indicated that there is no difference in the compositions of the CuNiTi wires with varying transition temperatures (Brantley & Eliades, 2001).

Simultaneously, Miura (1991) patented a thermally graded NiTi archwire wherein the posterior segments of the archwire corresponding to the molar region were heat

treated for about 5 minutes and the wire was progressively heat treated for longer periods of time in a salt bath with the premolar segment being subjected to heat treatment for approximately 15-60 minutes and the anterior segment for about 1-2.5 hours at a temperature of 500°C. This led to the introduction of the thermally graded nickel-titanium archwires or the BioForce archwires by GAC Dentsply (Kuftinec, 2008), which were based on the principle that the application of force and its influence on the amount of tooth movement is dependent on the root surface area of the tooth to be moved and its associated periodontal surface area. These heat treated nickel-titanium archwires varied in the amount of force applied across the entire archwire length with lighter forces in the anterior segment and progressively higher forces being imparted by the posterior segment of the archwire.

Yoneyama et al. (1993) conducted a study to investigate the influence of heat treatments in nitrate baths on the transformation temperature and bending properties of the Japanese NiTi wire and noted a reduction in transformation temperature with an increasing secondary treatment temperature. Also, the wires showed that the load deflection ratio decreased with increased treatment temperature and after treatment temperatures ranging between 460-540°C, the wires showed superelasticity with almost complete recovery following bending.

A Differential Scanning Calorimetric (DSC) study was conducted to compare the DERHT and direct hot air heat treatment methods of heat treatment and shaping NeoSentalloy archwires (Airoidi & Riva, 1995). The authors observed a non-uniform pattern of heat treatment by the DERHT method which reflected in the non-homogeneous

thermal behavior of the wire across different regions of the wires when treated by this method.

Other methods to produce wires which deliver graded force levels across the arch have also been tried and tested. However they have not met with much success. Below is a summary of some of these studies.

Sevilla et al. (2008) laser welded three different types of nickel-titanium wires of 0.45 mm diameter with compositions varying between 48.5 and 50 atomic% Ti and studied the mechanical performance, phase transformation behavior, corrosion properties and nickel release by these wires under simulated oral environment using a tensile test, differential scanning calorimetry, microstructural evaluation of the welded regions, corrosion test and ion release test. The authors surmised that, while welding did not influence the mechanical properties and transformation temperatures of the wire segments, it resulted in higher corrosion rates and ion release. Also, microstructural evaluation of the wires indicated that the welded regions were weak areas where tensile failure would be anticipated.

Gil et al. (2013) analyzed the influence of varying heat treatments in different segments of nickel-titanium wires on chemical composition, mechanical behavior and transformation temperatures in different zones within the same archwire. They first heat treated the wires to 900°C for 10 minutes followed by quenching the wires in water at 20°C, which resulted in stabilization of the austenitic phase of the wire at room temperature. This was followed by heat treating the posterior segment of the wire at 500°C and the lateral segment at 350°C for 1 hour, while the anterior segment was left at room temperature. They observed the presence of titanium rich precipitates in the

posterior segment and a small variation in the chemical composition of the posterior segment which resulted in a large decrease in transformation temperature and stress induced martensitic transformation at higher loads.

Ibe & Segner (1998) conducted a study which compared the load deflection characteristics and force levels delivered within different regions of the same arch of five commercial brands of variable force wires and a superelastic nickel-titanium wire using a beam bending test with three round posts at a temperature of 35°C. They concluded that the wires did exhibit reduced force levels in the incisor region as compared to the molar segment, and that the BioForce archwires (GAC, Dentsply, Islandia, NY, USA) and Titanol Triple Force (Forestadent, Pforzheim, Germany) archwires showed the greatest percentage reduction in intra-arch force levels and these forces were in the biologically acceptable range for different teeth. They opined that the use of multi-force level archwires would especially offer clinical advantage in the initial phase of fixed appliance treatment by minimizing the incidence of root resorption and improving patient comfort.

Ion Implanted NiTi Wires

In order to reduce the amount of friction, release of Ni ions, and improve the corrosion resistance of nickel-titanium wires, an ion implantation technique has been used which results in hardening the metallic substrate of the wire by bombardment of high energy ions, typically nitrogen. This results in a modification of the surface of the archwire and increase in surface hardness (Wichelhaus et al., 2005; Braga et al., 2011). IonGuard BioForce archwires (Dentsply GAC, Islandia, NY, USA) which have been ion-implanted are available for clinical use (Kuftinec, 2008). The ion implantation

process has been shown to improve friction associated with these wires when compared to the non-ion-implanted BioForce archwires, thus theoretically allowing lower forces to be applied to achieve tooth movement. However, clinical use of nickel-titanium wires has been shown to bring about a significant increase in the amount of friction associated with them (Wichelhaus et al., 2005).

Differential Scanning Calorimetry

Differential scanning calorimetry has been used to study the phase transformation behavior and the metallurgical structure of nickel-titanium archwires (Brantley & Eliades, 2001). Identification of the transition temperatures, transformation temperature ranges, and enthalpy changes associated with these wires has served to identify and correlate the phases present in the wires with their mechanical behavior. The three generations of nickel-titanium wires differ in their thermal behavior and the phases present at oral temperature, which in turn is one of the factors influencing their bending characteristics, superelastic behavior and stiffness when used clinically (Brantley & Eliades, 2001; Santoro et al., 2001). Differential scanning calorimetric studies have identified the presence of additional peaks during the heating/cooling curves, and have been attributed to the presence of an intermediate rhombohedral “R” phase. This phase maybe present in some proportion relative to the other two phases at oral temperatures.

Bradley et al. (1996) conducted a Differential Scanning Calorimetry study to reconcile reported differences amongst the transformation temperatures within austenitic, martensitic and rhombohedral phases of the commercial nitinol wires. The cooling scans going down to -170°C reported that while the transformation from austenitic to

martensitic was invariably associated with an intermediate R phase, the heating scans did not consistently display this character. Based on their temperature studies, they suggested different proportions of austenitic, martensitic and R phase phases amongst the commercial brands at typical oral temperatures. They also determined consistent enthalpy changes for most wires as reported in the literature then.

CHAPTER 3

MATERIALS AND METHODS

Five brands of variable force orthodontic wires, as listed in Table 1, were tested to evaluate their thermomechanical characteristics. All wires tested were of 0.016 X 0.016 inch and in as-received condition. For each wire brand, three separate subgroups—Anterior, Premolar, and Molar were evaluated and compared respectively to the same segments of NeoSentalloy (Dentsply GAC, Islandia, NY), a heat activated NiTi wire, as a non-variable force control.

Wire Brand	Manufacturer
BioForce	Dentsply GAC, Islandia, NY
BioForce IonGuard	Dentsply GAC, Islandia, NY
TriTanium	American Orthodontics, Sheboygan, WI
Titanol Triple Force	Forestadent, Pforzheim, Germany
Tri-Force Thermal	Masel Orthodontics, Carlston, CA
NeoSentalloy	Dentsply GAC, Islandia, NY

Table 1. Brand names and manufacturers of wires of different groups

The phase transformation characteristics of the wires were studied using Differential Scanning Calorimetry and load deflection behavior of the wires was examined using the three point bending test.

Differential Scanning Calorimetry

Ten specimens of 4 mm length sections representing the central region of the three subgroups, viz. anterior, premolar and molar, of all six groups were analyzed with differential scanning calorimetry (n=10/segment/brand). In order to obtain 4–5 mm anterior, premolar and molar segments of wire, they were sectioned from areas marked along the arch form, using the guide given in the BioForce archwire manufacturer's catalogue (Kuftinec, 2008).

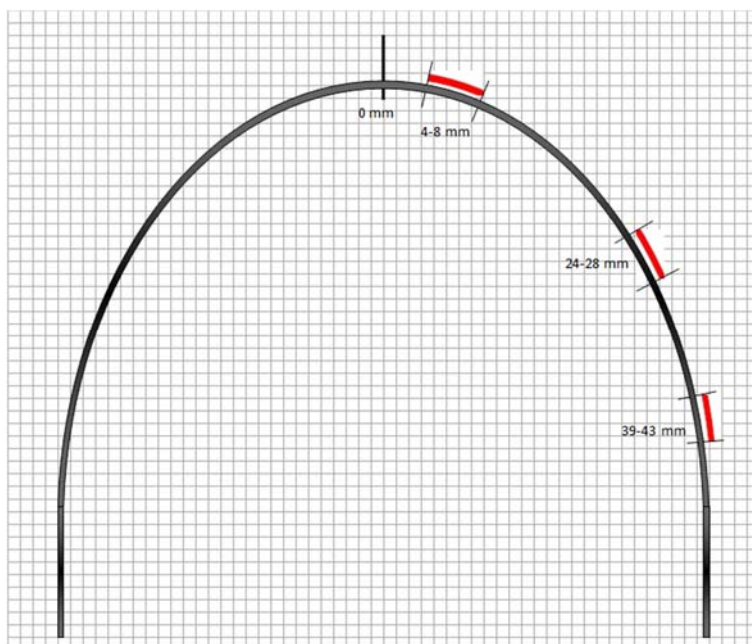


Figure 1. Illustration showing 4 mm segment samples as taken from the anterior, premolar and molar segments from the archwires for the DSC test (not to scale)

Sections of the central region of each segment were made with a low-speed, water-cooled diamond saw (Isomet, Buehler Ltd., Lake Bluff, IL). The specimens were weighed with an electronic weighing scale (Mettler-Toledo Inc., Columbus, OH) and then sealed in an aluminum crucible with a small hole punched into the cap of the crucible. An empty aluminum crucible was used as a reference. The specimens were tested in a DSC apparatus (Model 822e, Mettler-Toledo Inc., Columbus, OH) and

scanned by heating them from -100 to 100°C at the rate of $10^{\circ}\text{C}/\text{min}$ and then reversed, with liquid nitrogen as a coolant. The DSC graphs (thermograms) were obtained and analyzed using the DSC manufacturer's software to assess the heating and cooling curves. The onset, peak, and finish temperatures and enthalpy changes associated with phase transformations during the heating and cooling were obtained from the thermograms.

Three point bending test

The force delivered by the wires in the three regions was studied by using the three point bending test with a universal testing machine (Model 5500R, Instron Corp., Norwood, MA) at a temperature of $37\pm 2^{\circ}\text{C}$. Temperature was maintained with a portable heater. Twenty wires within each subgroup (anterior, premolar and molar) of each brand were tested ($n=20/\text{segment}/\text{brand}$). The test was conducted following ANSI/ADA Specification No. 32 (2006) as a guide. However, a fixture span of 14 mm was used instead of 10 mm prescribed in the specification due to a limitation of the fixture. Lengths of the anterior, premolar, and molar segments of wire (20 mm) were obtained as follows: the anterior and molar segments were obtained from one side of the archwire and the premolar segment was obtained from the opposite side so as obtain segments of adequate length which are representative of each region of the wire. The sections were made with a wire cutter. The wire segments were placed flatwise and subjected to a deflection of 3.1 mm at a cross-head speed of 2 mm/min and were unloaded at the same speed to their original position. The loading (activation) and unloading (deactivation) forces were recorded using custom software (Merlin, Instron Corp.). The stiffness was calculated by

measuring the slope of the linear portion of the curves and converted to modulus via the equation: $E = \text{stiffness} * L^3 / (4 b h^3)$ where L is the support span (14 mm), b is width (in mm), and h is thickness (in mm). Deflection loads (g) at 1, 2 and 3 mm of activation and deactivation were obtained from the data.

Statistical Analysis

The DSC and bending data were analyzed with a two-way ANOVA with brand of wire and segment (anterior, premolar, molar) as factors (SPSS 20, IBM Corp., Armonk, NY) and was followed by a post-hoc Dunnett's test ($p < 0.05$) in order to evaluate any statistically significant difference between the various brands and the control group (NeoSentalloy). A post-hoc Tukey's test was utilized to analyze differences between the three segments within each brand.

CHAPTER 4

RESULTS

Differential Scanning Calorimetry

Figures 2 to 7 demonstrate representative thermograms of the Anterior, Premolar and Molar segments of each of the six groups of orthodontic archwires. The thermograms show both heating and cooling curves for each brand of wire. The peaks represent the heat transfer associated with phase changes exhibited by the wires when heated and cooled. All wires demonstrated single peaks in the heating curve (except Titanol Triple Force) and two peaks in the cooling curve. The peaks are characterized by an onset temperature, a peak temperature, endset temperature and enthalpy change during phase transformation. The single peak in the heating curve represents the A_s and A_f temperatures of the wires, while the cooling curves demonstrate the presence of an intermediate R phase which is represented by the first peak (austenite to R phase) and the martensitic (R phase to martensite) phase transformation is represented by the second peak in the cooling curve.

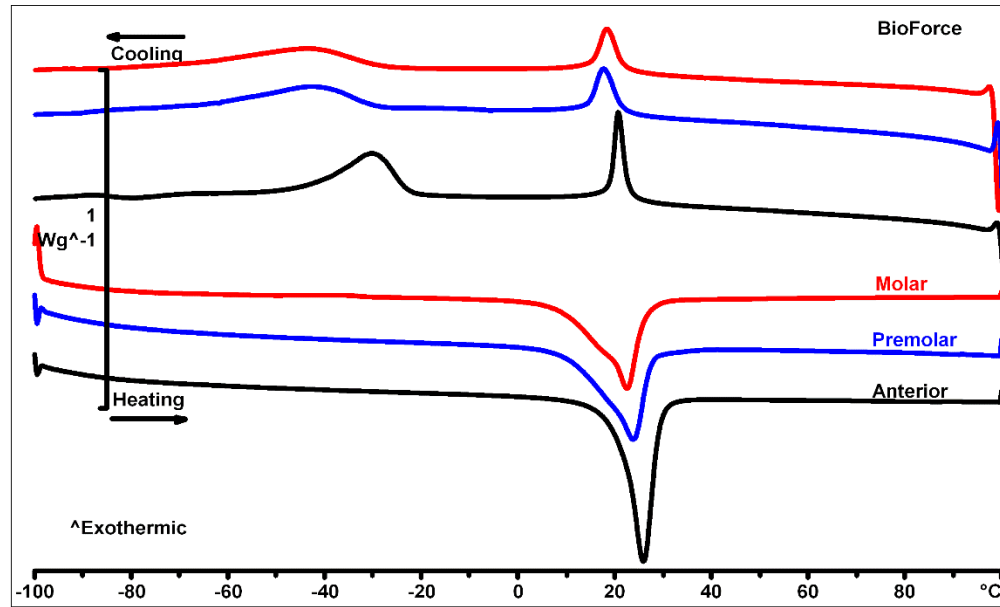


Figure 2. DSC heating and cooling curves of Anterior, Premolar and Molar segments of BioForce orthodontic wires

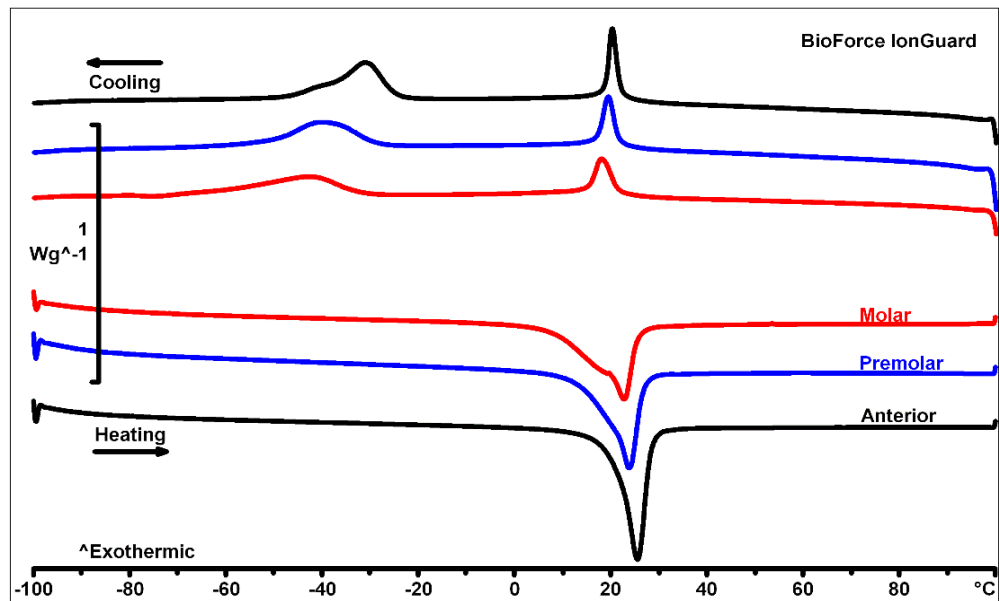


Figure 3. DSC heating and cooling curves of Anterior, Premolar and Molar segments of IonGuard BioForce orthodontic wires

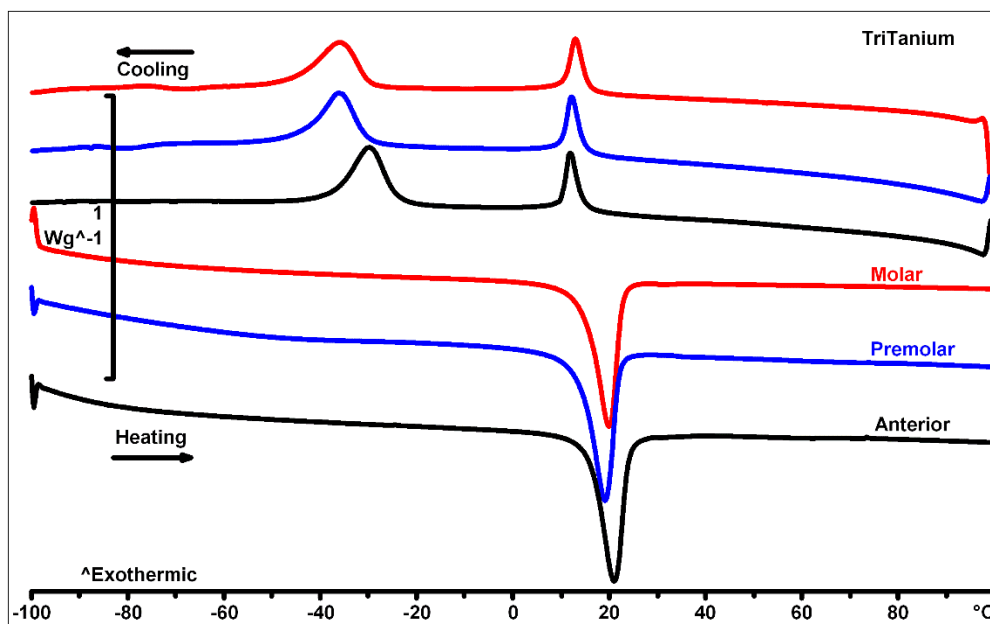


Figure 4. DSC heating and cooling curves of Anterior, Premolar and Molar segments of TriTanium orthodontic wires

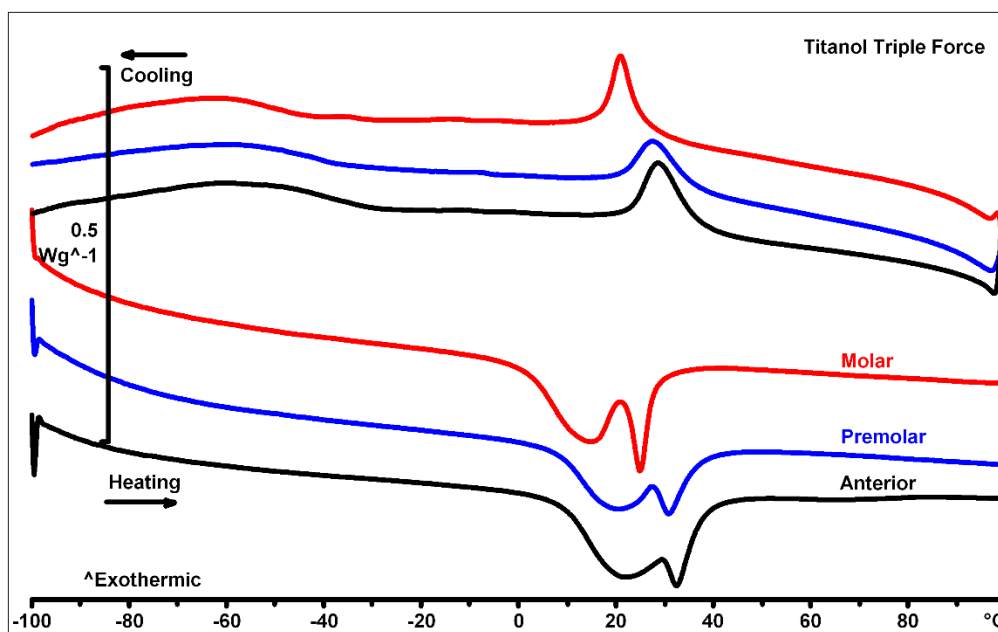


Figure 5. DSC heating and cooling curves of Anterior, Premolar and Molar segments of Titanol Triple Force orthodontic wires

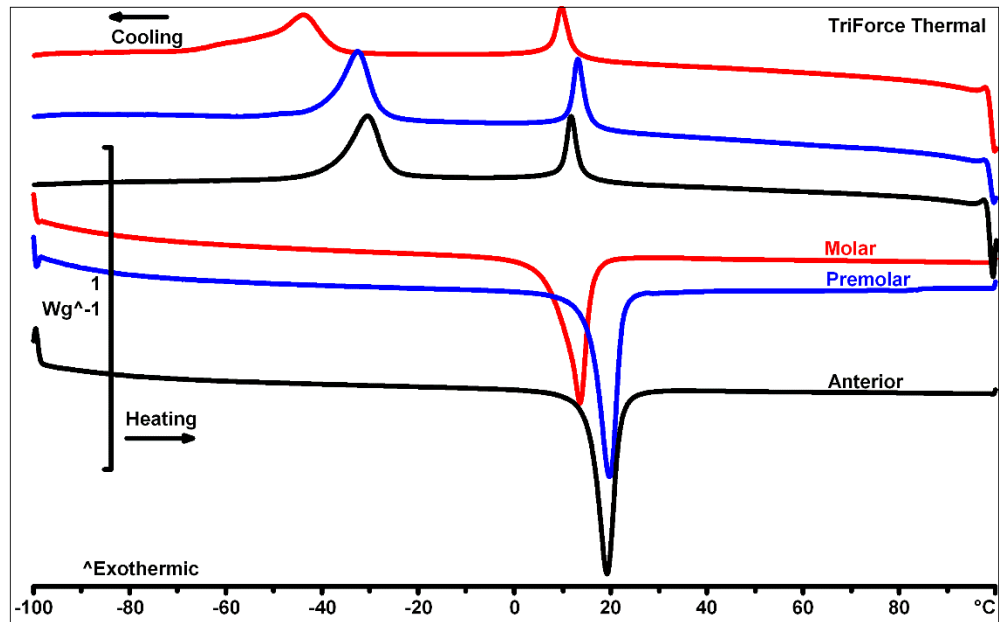


Figure 6. DSC heating and cooling curves of Anterior, Premolar and Molar segments of Tri-Force Thermal orthodontic wires

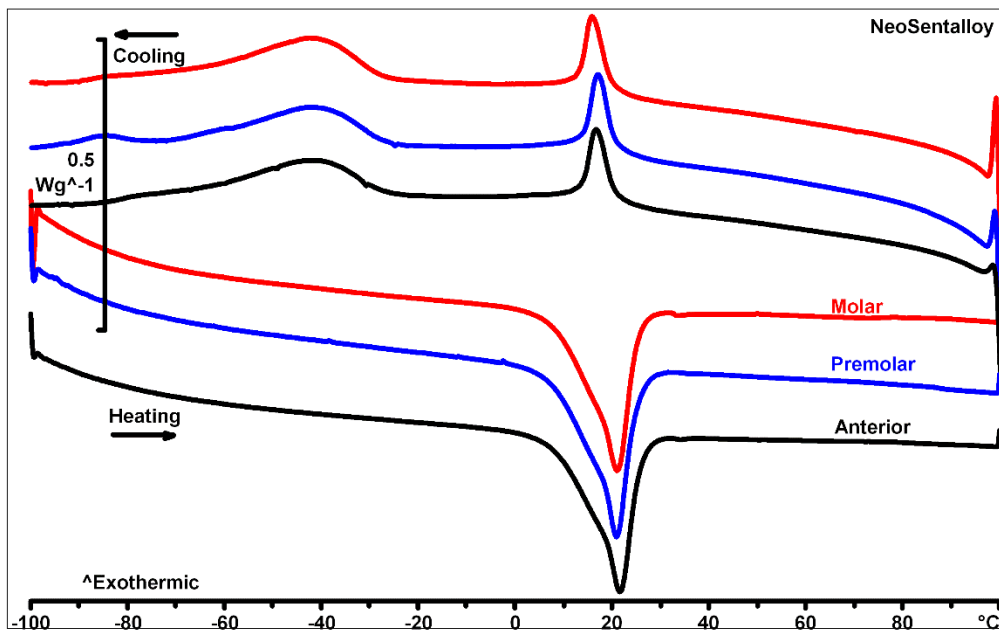


Figure 7. DSC heating and cooling curves of Anterior, Premolar and Molar segments of NeoSentallooy orthodontic wires

Figures 8 to 10 display thermograms reflecting anterior, premolar and molar segments of all six brands of the wires, respectively. The BioForce, IonGuard BioForce and Titanol groups of wires demonstrate peaks at higher temperatures as compared to the NeoSentalloy control group in the anterior and premolar segments.

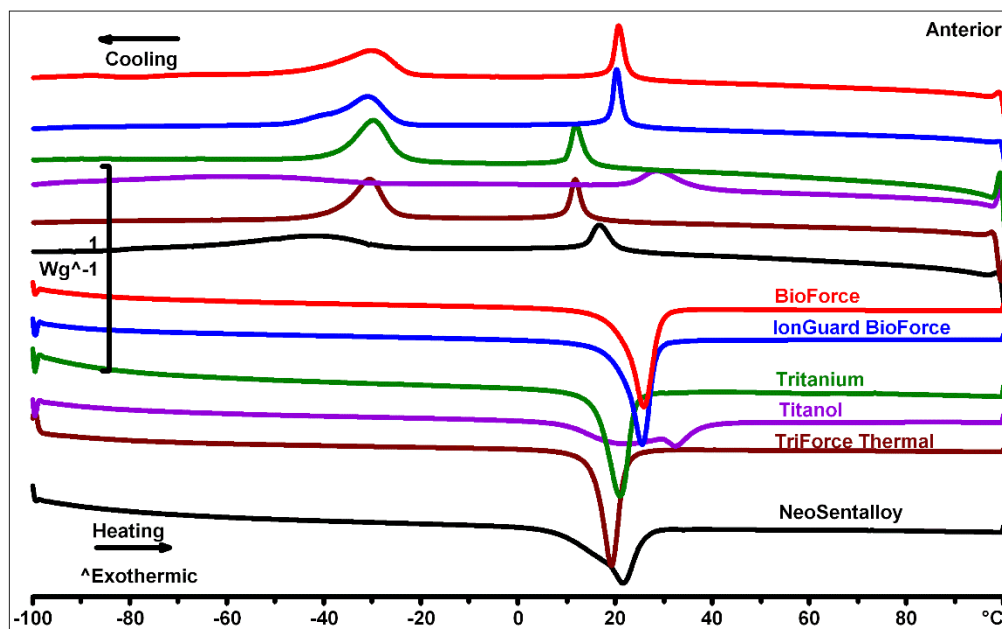


Figure 8. DSC heating and cooling curves of Anterior segments of six groups of wires

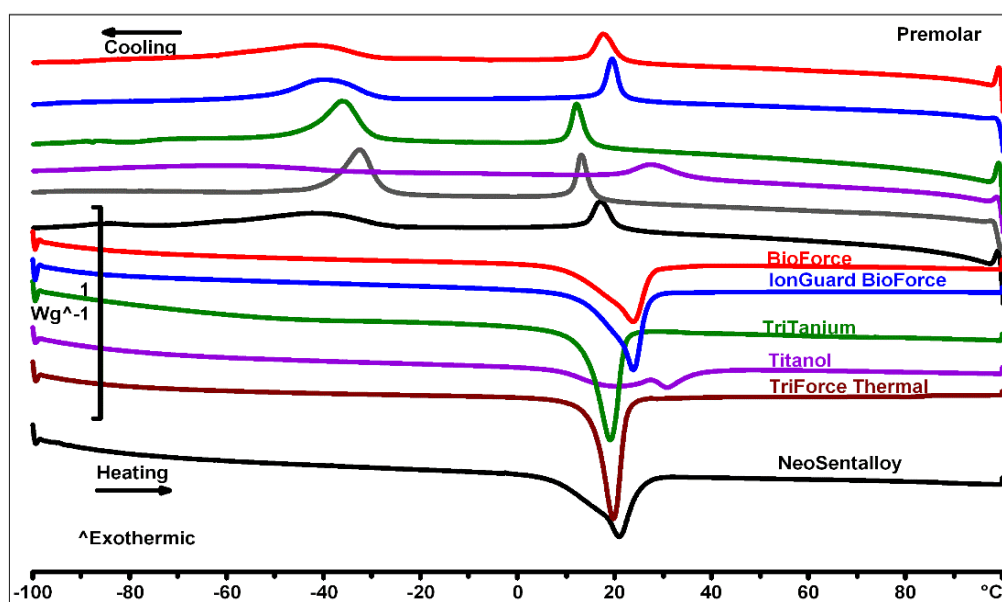


Figure 9. DSC heating and cooling curves of Premolar segments of six groups of wires

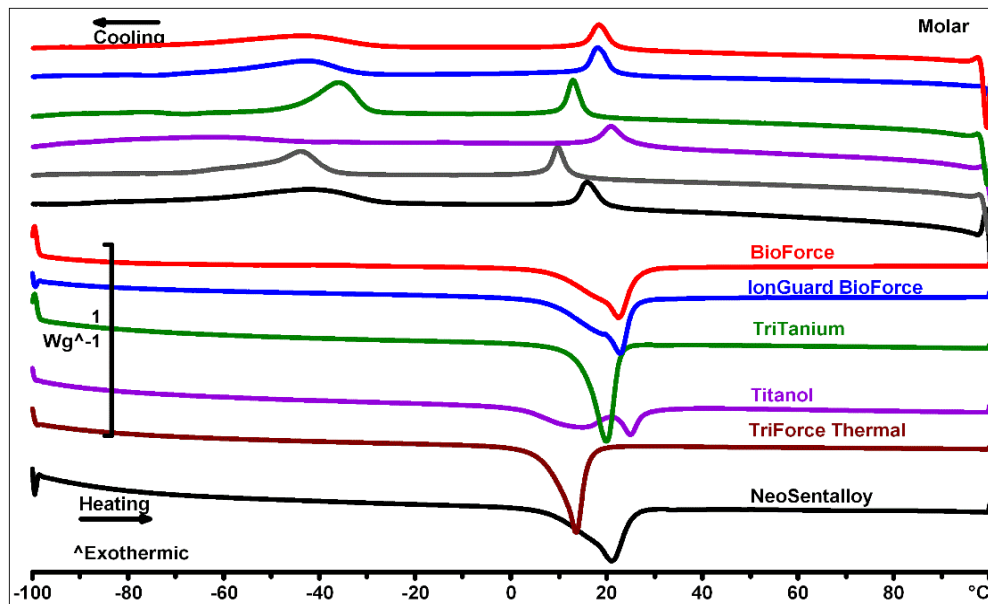


Figure 10. DSC heating and cooling curves of Molar segments of six groups of wires

Tables 2-3 display mean transformation temperatures and enthalpy changes associated with heating in the DSC test. The Anterior and Premolar segments show higher austenitic temperatures as compared to the Molar segments for the variable force archwires, while the NeoSentalloy wires show near constant values across the three segments. A comparison between the five variable force brands for the three segments displayed that the Titanol Triple Force wires exhibited the highest values for A_f temperature, while the Tri-Force Thermal archwires recorded the lowest values.

Wire Brand	Wire Segment	Heating			
		A _s temp (°C)	Peak temp (°C)	A _r temp (°C)	Enthalpy (J/g)
BioForce	Anterior	21.2±0.3 ^{a*}	26.7±0.6 ^{a*}	30.2±0.5 ^{a*}	17.48±0.79 ^{a*}
	Premolar	18.3±2.0 ^{b*}	24.2±1.2 ^{b*}	27.5±1.2 ^{b*}	14.24±2.41 ^b
	Molar	16.8±0.5 ^{c*}	22.5±0.7 ^c	25.9±0.7 ^c	12.27±1.61 ^{c*}
IonGuard BioForce	Anterior	21.4±2.4 ^{d*}	26.0±2.5 ^{d*}	29.4±2.8 ^{d*}	15.91±3.31 ^{d*}
	Premolar	20.7±0.9 ^{d*}	25.4±0.9 ^{d*}	28.6±1.0 ^{d*}	14.89±0.93 ^d
	Molar	16.7±2.4 ^{e*}	22.8±0.8 ^{e*}	25.8±1.0 ^e	12.19±2.41 ^{e*}
TriTanium	Anterior	18.2±1.6 ^{g*}	22.6±1.8 ^g	25.5±1.9 ^g	14.30±1.30 ^{h*}
	Premolar	17.0±2.0 ^{g*}	21.5±2.1 ^g	24.4±2.1 ^g	13.84±1.42 ^h
	Molar	11.8±3.7 ^h	17.7±2.4 ^{h*}	20.5±2.5 ^{h*}	16.24±1.07 ^g
Titanol	Anterior	7.4±1.4 ^{j*}	32.3±1.5 ^{j*}	38.0±1.2 ^{j*}	11.88±1.32 ^j
	Premolar	6.7±2.0 ^{j*}	30.0±2.7 ^{j*}	35.8±3.1 ^{j*}	11.85±1.27 ^{j*}
	Molar	1.8±1.6 ^{k*}	23.7±2.6 ^{k*}	27.9±3.4 ^{k*}	10.48±1.50 ^j
Tri-Force Thermal	Anterior	15.6±1.9 ^m	19.7±2.3 ^m	22.7±2.5 ^{m*}	13.91±1.38 ^{m*}
	Premolar	15.0±1.3 ^m	19.0±1.4 ^{m*}	22.0±1.6 ^{m*}	15.38±2.09 ^m
	Molar	9.9±3.5 ^{m*}	15.1±2.5 ^{n*}	17.9±2.5 ^{n*}	15.04±1.49 ^m
NeoSentalloy	Anterior	14.9±0.6 ^{p,q}	21.1±0.7 ^p	25.2±0.7 ^p	12.43±0.67 ^p
	Premolar	15.0±0.7 ^p	21.3±0.7 ^p	25.4±0.8 ^p	13.21±2.67 ^p
	Molar	13.4±2.1 ^q	20.4±2.0 ^p	25.0±0.7 ^p	16.22±5.83 ^p

Table 2. DSC measured Austenitic temperatures and enthalpy changes for phase transformations in the heating within three segments for all six groups of wires (* represents a significant difference of the other brands from NeoSentalloy; different letters denote significance differences between the segments for a given wire brand)

Wire Segment	Wire Brand	Heating			
		A _s temp (°C)	Peak temp (°C)	A _f temp (°C)	Enthalpy (J/g)
Anterior	BioForce	21.2±0.3 ^A	26.7±0.6 ^B	30.2±0.5 ^B	17.48±0.79 ^A
	IonGuard BioForce	21.4±2.4 ^A	26.0±2.5 ^B	29.4±2.8 ^B	15.91±3.31 ^{A,B}
	TriTanium	18.2±1.6 ^B	22.6±1.8 ^C	25.5±1.9 ^C	14.30±1.30 ^B
	Titanol Triple Force	7.4±1.4 ^D	32.3±1.5 ^A	38.0±1.2 ^A	11.88±1.32 ^C
	Tri-Force Thermal	15.6±1.9 ^C	19.7±2.3 ^D	22.7±2.5 ^D	13.91±1.38 ^{B,C}
Premolar	BioForce	18.3±2.0 ^G	24.2±1.2 ^G	27.5±1.2 ^G	14.24±2.41 ^F
	IonGuard BioForce	20.7±0.9 ^F	25.4±0.9 ^G	28.6±1.0 ^G	14.89±0.93 ^F
	TriTanium	17.0±2.0 ^{G,H}	21.5±2.1 ^H	24.4±2.1 ^H	13.84±1.42 ^{F,G}
	Titanol Triple Force	6.7±2.0 ^I	30.0±2.7 ^F	35.8±3.1 ^F	11.85±1.27 ^G
	Tri-Force Thermal	15.0±1.3 ^H	19.0±1.4 ^I	22.0±1.6 ^H	15.38±2.09 ^F
Molar	BioForce	16.8±0.5 ^K	22.5±0.7 ^K	25.9±0.7 ^K	12.27±1.61 ^L
	IonGuard BioForce	16.7±2.4 ^K	22.8±0.8 ^K	25.8±1.0 ^K	12.19±2.41 ^L
	TriTanium	11.8±3.7 ^L	17.7±2.4 ^L	20.5±2.5 ^L	16.24±1.07 ^K
	Titanol Triple Force	1.8±1.6 ^M	23.7±2.6 ^K	27.9±3.4 ^K	10.48±1.50 ^L
	Tri-Force Thermal	9.9±3.5 ^L	15.1±2.5 ^M	17.9±2.5 ^L	15.04±1.49 ^K

Table 3. Comparison of DSC measured Austenitic temperatures and enthalpy changes for phase transformation during heating within the three segments for five brands of variable force wires (Different letters denote significant differences between the brands for a given segment)

Tables 4-5 display mean transformation temperatures and enthalpy changes associated with cooling in the DSC test. The cooling curves exhibit an intermediate transformation peak to the R phase at temperatures ranging between 11-25°C and a martensitic transformation at lower temperatures for all the wires and segments.

Wire Brand	Wire Segment	Cooling							
		Peak 1				Peak 2			
		R _s temp (°C)	Peak temp (°C)	R _f temp (°C)	Enthalpy (J/g)	M _s temp (°C)	Peak temp (°C)	M _f temp (°C)	Enthalpy (J/g)
BioForce	Anterior	22.7 ±0.4 ^{a*}	20.2 ±0.6 ^{a*}	18.2 ±0.6 ^{a*}	4.46 ±0.19 ^a *	-23.1 ±1.2 ^{a*}	-31.4 ±1.0 ^{a*}	-43.9 ±2.0 ^{a*}	8.74 ±0.99 [*]
	Premolar	22.2 ±0.4 ^{a*}	19.3 ±0.8 ^{b*}	16.6± 1.1 ^{b*}	3.8± 0.35 ^b	-27.6± 2.0 ^b	-38.1 ±3.2 ^b	-54.4 ±5.2 ^b	6.26 ±0.81 ^b *
	Molar	22.2 ±0.6 ^{a*}	18.7 ±0.5 ^{b*}	15.8 ±0.5 ^{b*}	3.82 ±0.16 ^b	-30.4 ±1.0 ^c	-43.8 ±3.0 ^c	-64.1 ±3.3 ^c	5.29 ±2.29 ^b
IonGuard BioForce	Anterior	22.8 ±4.1 ^{d*}	20.1 ±2.8 ^{d*}	18.0 ±2.5 ^{d*}	4.16 ±0.60 ^d	-24.0 ±2.3 ^{d*}	-31.6 ±1.1 ^{d*}	-41.2 ±1.6 ^{d*}	8.23 ±1.72 ^d
	Premolar	22.2 ±0.8 ^{d*}	20.0 ±0.9 ^{d*}	18.2 ±1.0 ^{d*}	3.78 ±0.38 ^{de}	-26.2 ±1.6 ^d	-35.3 ±2.3 ^{e*}	-46.8 ±2.5 ^{e*}	7.02 ±1.42 ^d *
	Molar	22.3 ±2.1 ^{d*}	18.5 ±1.0 ^{d*}	15.5 ±1.1 ^{e*}	3.38 ±0.78 ^e *	-33.6 ±2.5 ^{e*}	-45.2 ±3.3 ^f	-56.1 ±4.1 ^f	4.49 ±1.84 ^e *
TriTanium	Anterior	16.2 ±0.9 ^{g*}	13.5 ±1.1 ^{g*}	11.5 ±1.0 ^{gh*}	4.03 ±0.19 ^g	-22.5 ±2.9 ^{g*}	-27.6 ±2.7 ^{g*}	-34.5 ±2.7 ^{g*}	9.29 ±0.91 ^g *
	Premolar	16.5 ±1.9 ^{g*}	13.8 ±1.6 ^{g*}	13.0 ±3.5 ^g	3.35 ±0.57 ^h	-25.5 ±4.4 ^g	-31.8 ±5.7 ^{g*}	-39.5 ±9.0 ^{g*}	8.47 ±1.84 ^g *
	Molar	14.6 ±1.4 ^{h*}	11.8 ±1.7 ^{h*}	9.4 ±1.7 ^{h*}	3.37 ±0.29 ^h *	-33.3 ±4.6 ^{h*}	-39.4 ±4.5 ^h	-48.5 ±4.7 ^{h*}	5.32 ±2.0 ^h
Titanol	Anterior	36.5 ±0.9 ⁱ	28.9 ±1.4 [*]	22.8 ±1.6 [*]	3.74 ±0.36 ^j	-35.1 ±2.7 ^{j*}	-55.3 ±3.9 ^{j*}	-74.5 ±9.4 [*]	2.81 ±0.66 ^j *
	Premolar	33.6 ±3.6 ^j	25.9 ±4.3 [*]	19.7 ±4.8 ^{j,k*}	3.0 ±0.66 ^{j,k}	-38.0 ±4.6 ^{j*}	-56.1 ±3.8 ^{i,h*}	-76.1 ±11.2 ^j *	2.74 ±1.8 [*]
	Molar	25.2 ±2.8 ^k	20.4 ±1.8 ^{k*}	16.6 ±1.8 ^{k*}	3.2 ±0.43 ^k *	-45.9 ±2.8 ^{k*}	-59.3 ±3.1 ^{j*}	-73.8 ±10.7 ^j *	1.93 ±0.91 ^j *
Tri-Force Thermal	Anterior	14.3 ±0.8 ^m	12.0 ±0.9 ^{m*}	10.1 ±1.0 ^{m*}	2.71 ±0.26 ^m *	-24.9 ±4.7 ^{m*}	- 30.2 ^{m*}	-37.0 ±4.4 ^{m*}	7.29 ±1.41 ^m
	Premolar	14.4 ±0.7 ^{m*}	12.2 ±0.7 ^{m*}	10.2 ±0.6 ^{m*}	2.82 ±0.32 ^m *	-26.5 ±3.7 ^m	-31.5 ±3.4 ^{m*}	-38.2 ±3.2 ^j m*	7.23 ±0.8 ^{m*}
	Molar	11.8 ±2.0 ^{n*}	9.0 ±2.6 ^{n*}	6.6 ±3.1 ^{n*}	2.63 ±0.38 ^m *	-34.0 ±5.5 ^{n*}	-40.4 ±6.0 ⁿ	-49.5 ±7.2 ⁿ	8.12 ±1.00 ^m
Neo Sentalloy	Anterior	20.4 ±0.2 ^p	16.6 ±0.2 ^p	13.6 ±0.2 ^p	4.09 ±0.43 ^p	-28.8 ±3.6 ^p	-41.6 ±1.5 ^p	-59.9 ±3.1 ^q	7.24 ±0.57 ^p
	Premolar	20.2 ±0.2 ^p	16.5 ±0.5 ^p	13.6 ±0.5 ^p	3.49 ±0.32 ^q	-28.4 ±0.8 ^p	-41.1 ±2.3 ^p	-56.9 ±2.0 ^p	4.68 ±0.30 ^r
	Molar	20.5 ±0.3 ^p	16.7 ±0.5 ^p	13.7 ±0.5 ^p	3.94 ±0.29 ^p	-27.8 ±0.4 ^p	-41.2 ±1.1 ^p	61.3 ±1.3 ^q	6.5 ±0.92 ^q

Table 4. DSC measured R phase and martensitic temperatures, and enthalpy for phase transformation during cooling in the six groups (* represents a significant difference of the other brands from NeoSentalloy; different letters denote significance differences between the segments for a given wire brand)

Wire Segment	Wire Brand	Cooling							
		R _s temp (°C)	Peak temp (°C)	R _f temp (°C)	Enthalpy (J/g)	M _s temp (°C)	Peak temp (°C)	M _f temp (°C)	Enthalpy (J/g)
		Peak 1				Peak 2			
Anterior	BioForce	22.7 ±0.4 ^B	20.2 ±0.6 ^B	18.2 ±0.6 ^B	4.46 ±0.19 ^A	-23.1 ±1.2 ^A	-31.4 ±1.0 ^B	-43.9 ±2.0 ^C	8.74 ±0.99 ^{A, B}
	IonGuard BioForce	22.8 ±4.1 ^B	20.1 ±2.8 ^B	18.0 ±2.5 ^B	4.16 ±0.60 ^{A, B}	-24.0 ±2.3 ^A	-31.6 ±1.1 ^B	-41.2 ±1.6 ^{B,C}	8.23 ±1.72 ^{A, B}
	TriTanium	16.2 ±0.9 ^C	13.5 ±1.1 ^C	11.5 ±1.0 ^C	4.03 ±0.19 ^{A, B}	-22.5 ±2.9 ^A	-27.6 ±2.7 ^A	-34.5 ±2.7 ^A	9.29 ±0.91 ^A
	Titanol Triple Force	36.5 ±0.9 ^A	28.9 ±1.4 ^A	22.8 ±1.6 ^A	3.74 ±0.36 ^B	-35.1 ±2.7 ^B	-55.3 ±3.9 ^C	-74.5 ±9.4 ^D	2.81 ±0.66 ^C
	Tri-Force Thermal	14.3 ±0.8 ^C	12.0 ±0.9 ^C	10.1 ±1.0 ^C	2.71 ±0.26 ^C	-24.9 ±4.7 ^A	-	-37.0 ±4.4 ^{A,B}	7.29 ±1.41 ^B
Premolar	BioForce	22.2 ±0.4 ^G	19.3 ±0.8 ^G	16.6 ±1.1 ^F	3.8 ±0.35 ^F	-27.6 ±2.0 ^F	-38.1 ±3.2 ^G	-54.4 ±5.2 ^G	6.26 ±0.81 ^G
	IonGuard BioForce	22.2 ±0.8 ^G	20.0 ±0.9 ^G	18.2 ±1.0 ^F	3.78 ±0.38 ^F	-26.2 ±1.6 ^F	-35.3 ±2.3 ^{F,G}	-46.8 ±2.5 ^{F,G}	7.02 ±1.42 ^{F, G}
	TriTanium	16.5 ±1.9 ^H	13.8 ±1.6 ^H	13.0 ±3.5 ^G	3.35 ±0.57 ^{F, G}	-25.5 ±4.4 ^F	-31.8 ±5.7 ^F	-39.5 ±9.0 ^F	8.47 ±1.84 ^F
	Titanol Triple Force	33.6 ±3.6 ^F	25.9 ±4.3 ^F	19.7 ±4.8 ^F	3.0 ±0.66 ^G	-38.0 ±4.6 ^G	-56.1 ±3.8 ^H	-76.1 ±11.2 ^H	2.74 ±1.8 ^H
	Tri-Force Thermal	14.4 ±0.7 ^H	12.2 ±0.7 ^H	10.2 ±0.6 ^G	2.82 ±0.32 ^G	-26.5 ±3.7 ^F	-31.5 ±3.4 ^F	-38.2 ±3.2 ^F	7.23 ±0.87 ^{F, G}
Molar	BioForce	22.2 ±0.6 ^L	18.7 ±0.5 ^K	15.8 ±0.5 ^K	3.82 ±0.16 ^K	-30.4 ±1.0 ^K	-43.8 ±3.0 ^{K,L}	-64.1 ±3.3 ^L	5.29 ±2.29 ^L
	IonGuard BioForce	22.3 ±2.1 ^L	18.5 ±1.0 ^K	15.5 ±1.1 ^K	3.38 ±0.78 ^{K, L}	-33.6 ±2.5 ^K	-45.2 ±3.3 ^L	-56.1 ±4.1 ^{K,L}	4.49 ±1.84 ^L
	TriTanium	14.6 ±1.4 ^M	11.8 ±1.7 ^L	9.4 ±1.7 ^L	3.37 ±0.29 ^{K, L}	-33.3 ±4.6 ^K	-39.4 ±4.5 ^K	-48.5 ±4.7 ^K	5.32 ±2.0 ^L
	Titanol Triple Force	25.2 ±2.8 ^K	20.4 ±1.8 ^K	16.6 ±1.8 ^K	3.2 ±0.43 ^{L, M}	-45.9 ±2.8 ^L	-59.3 ±3.1 ^M	-73.8 ±10.7 ^M	1.93 ±0.91 ^M
	Tri-Force Thermal	11.8 ±2.0 ^N	9.0 ±2.6 ^M	6.6 ±3.1 ^M	2.63 ±0.38 ^M	-34.0 ±5.5 ^K	-40.4 ±6.0 ^{K,L}	-49.5 ±7.2 ^K	8.12 ±1.00 ^K

Table 5. Comparison of DSC measured R phase and Martensitic temperatures, and enthalpy changes for phase transformation during cooling within the three segments for five brands of variable force wires (Different letters denote significant differences between the brands for a given segment)

Three point bending

Figures 11-16 represent representative load-deflection curves of the Anterior, Premolar and Molar segments of each of the six brands of wires. The load-deflection curves show a linear portion representing the elastic region in the loading and unloading region with a horizontal plateau representing the constant load levels during activation and deactivation of the wires with hysteresis in the activation/deactivation loads. The five variable brand wires show lower loads delivered for the same amount of activation in the anterior and premolar region as compared to the molar region, while the NeoSentalloy wires show near constant levels of load delivered between the three regions, as is seen in the overlapping of the three curves in Figure 16.

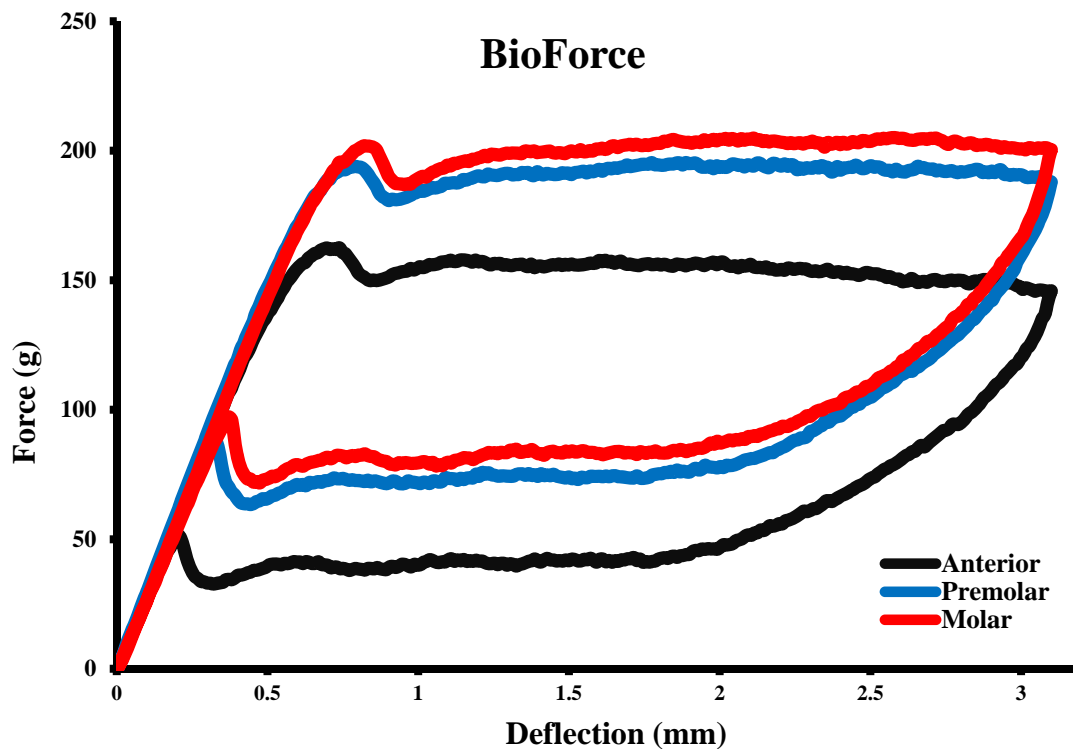


Figure 11. Force deflection curves for Anterior, Premolar and Molar segments of BioForce wires

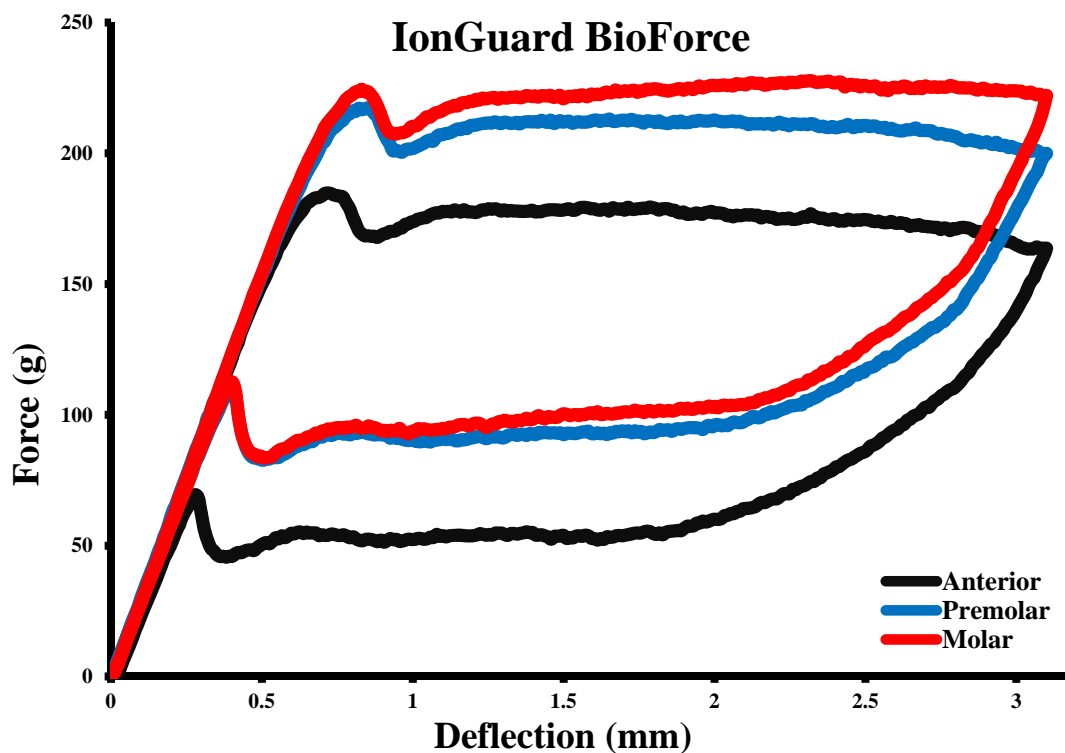


Figure 12. Force deflection curves for Anterior, Premolar and Molar segments of IonGuard BioForce wires

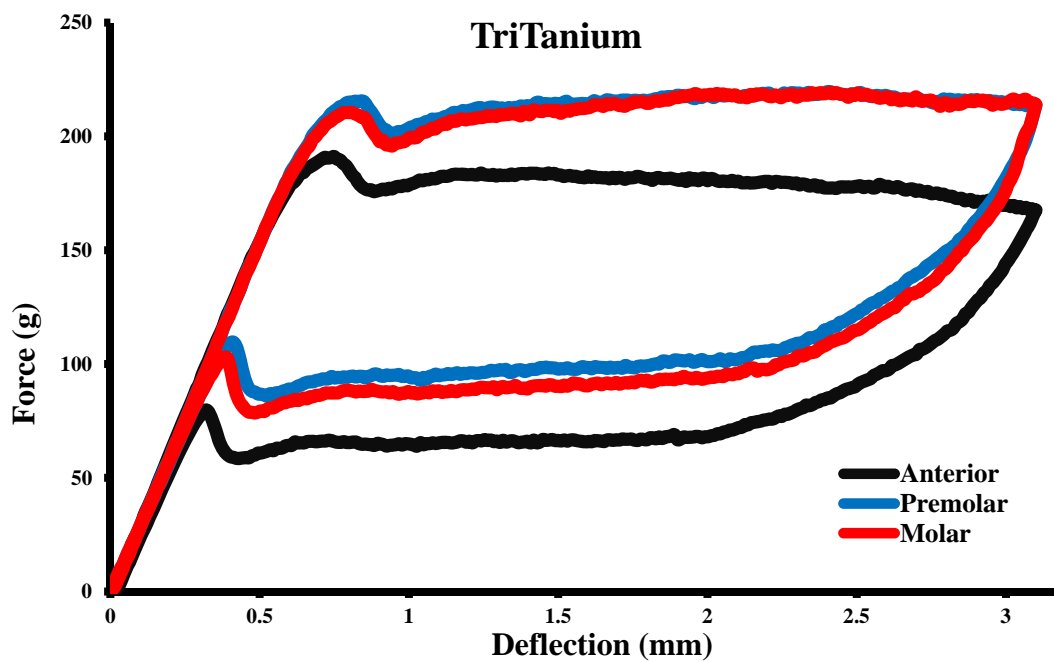


Figure 13. Force deflection curves for Anterior, Premolar and Molar segments of TriTanium wires

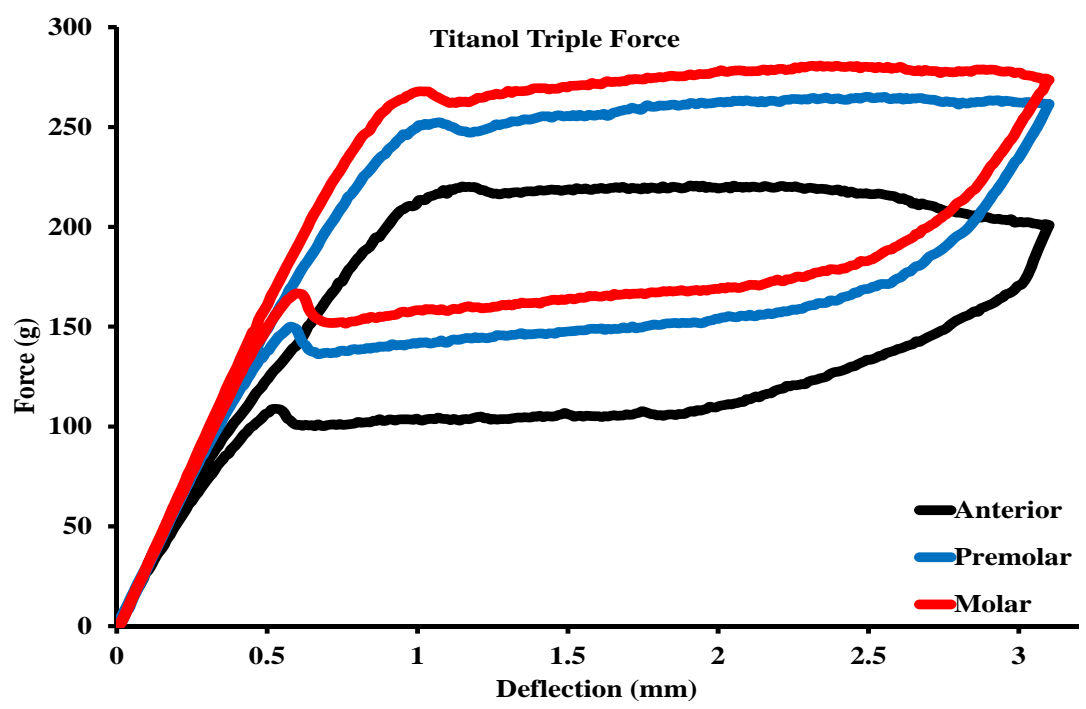


Figure 14. Force deflection curves for Anterior, Premolar and Molar segments of Titanol Triple Force wires

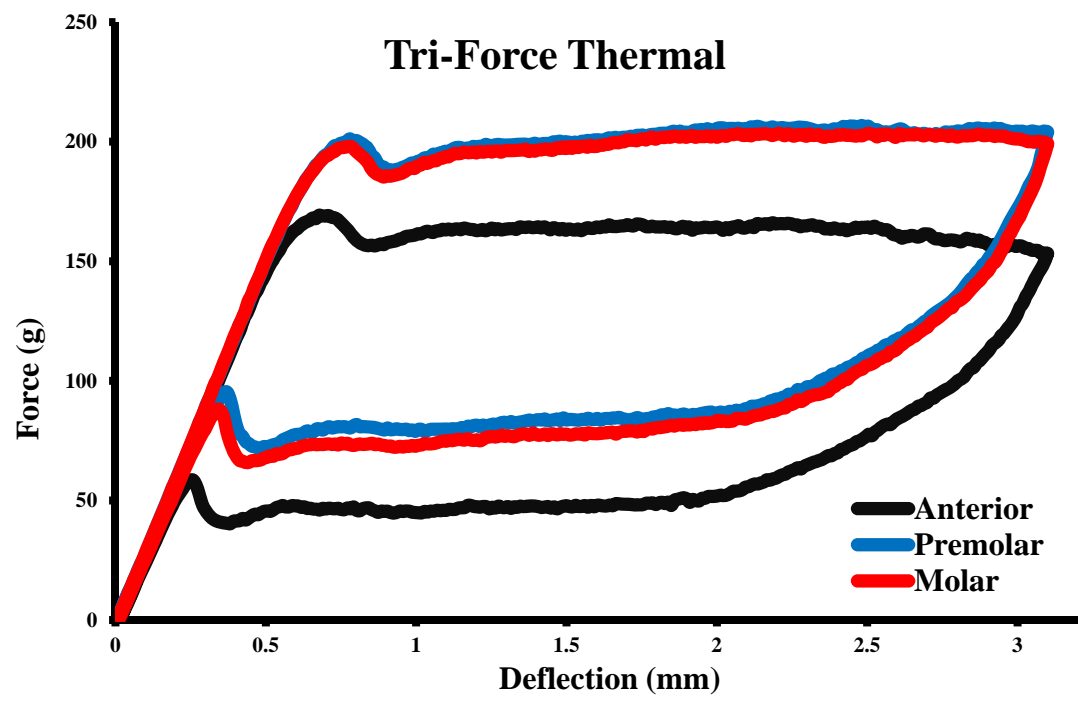


Figure 15. Force deflection curves for Anterior, Premolar and Molar segments of Tri-Force Thermal wires

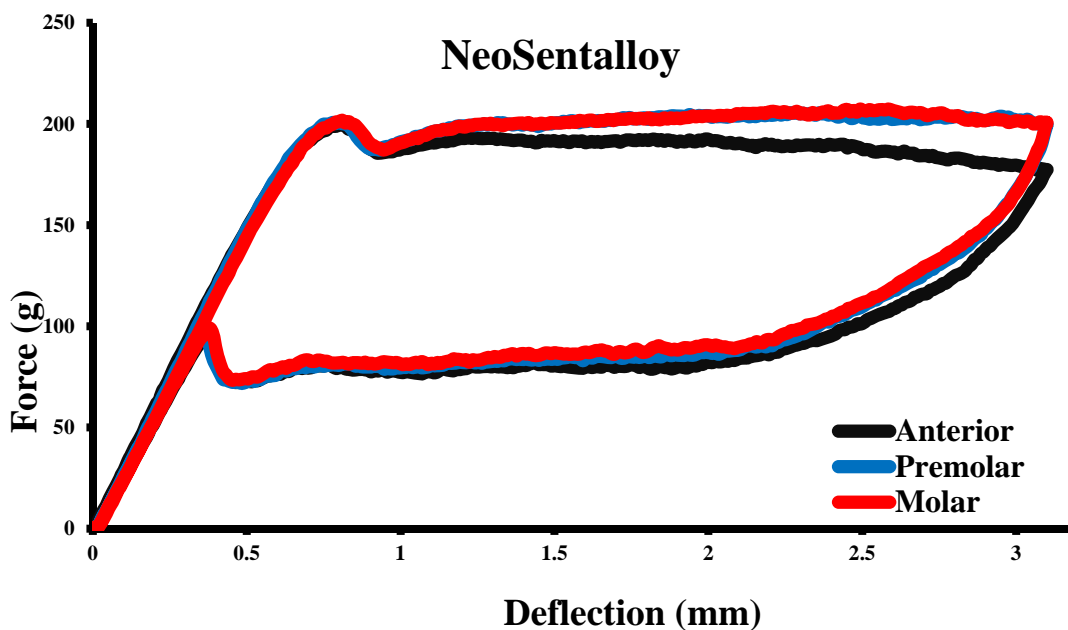


Figure 16. Force deflection curves for Anterior, Premolar and Molar segments of NeoSentalloy wires

Figures 17-19 reflect a comparison of the load-deflection curves of the anterior, premolar and molar segments of the six groups of wires. Appreciable differences in force values are apparent.

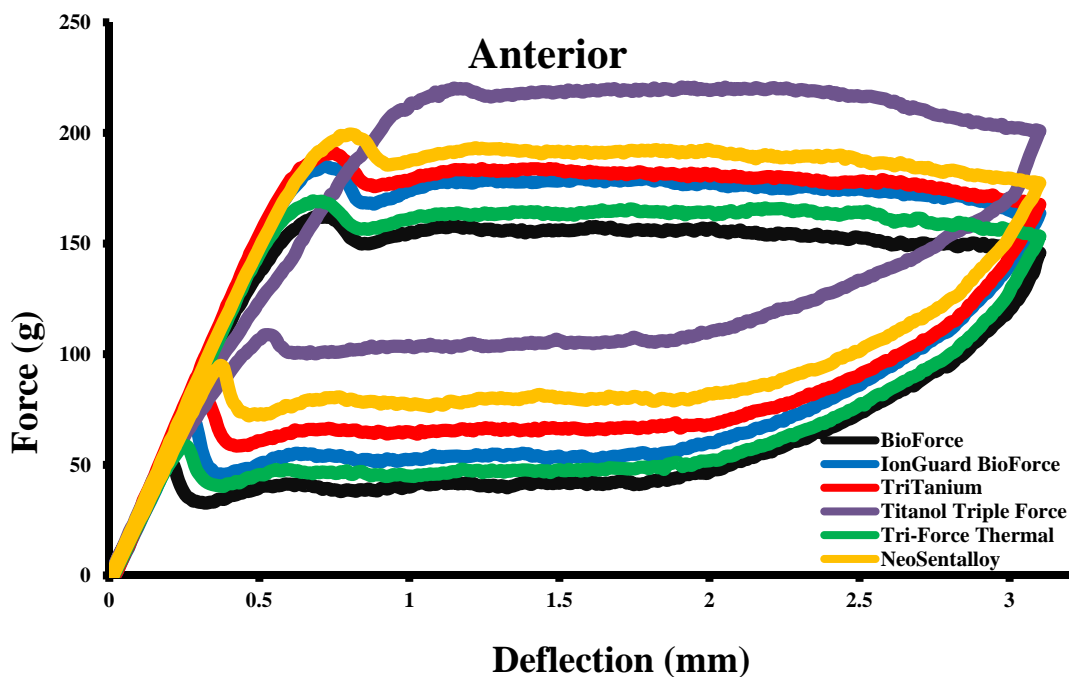


Figure 17. Force deflection curves for Anterior segment of six brands of wires

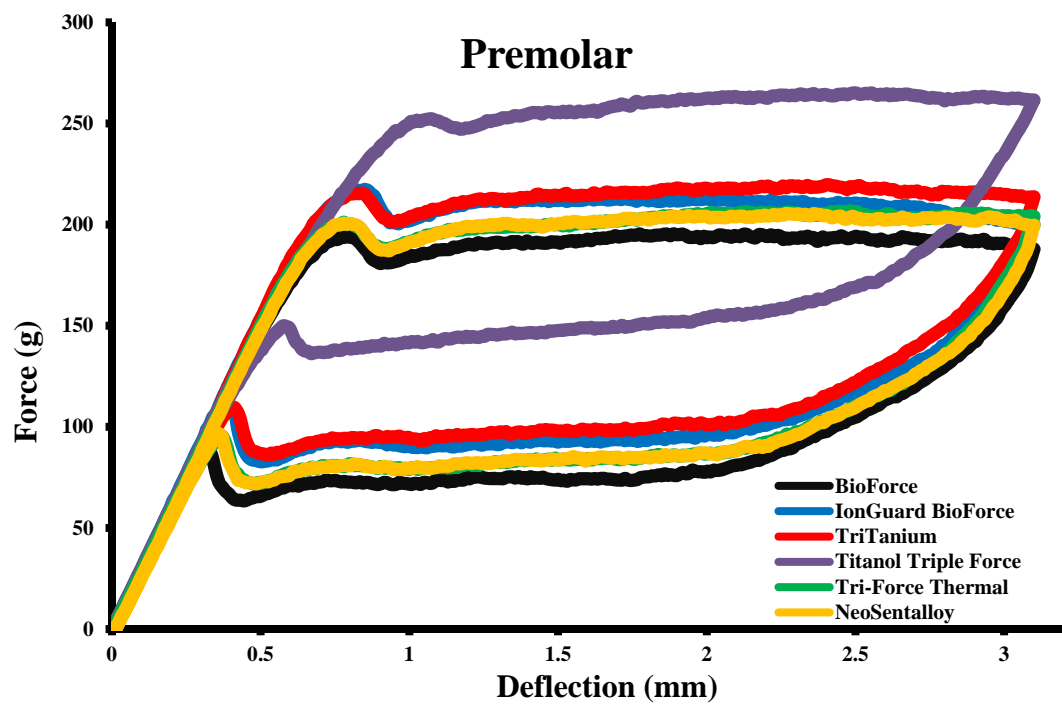


Figure 18. Force deflection curves of Premolar segment of six brands of wires

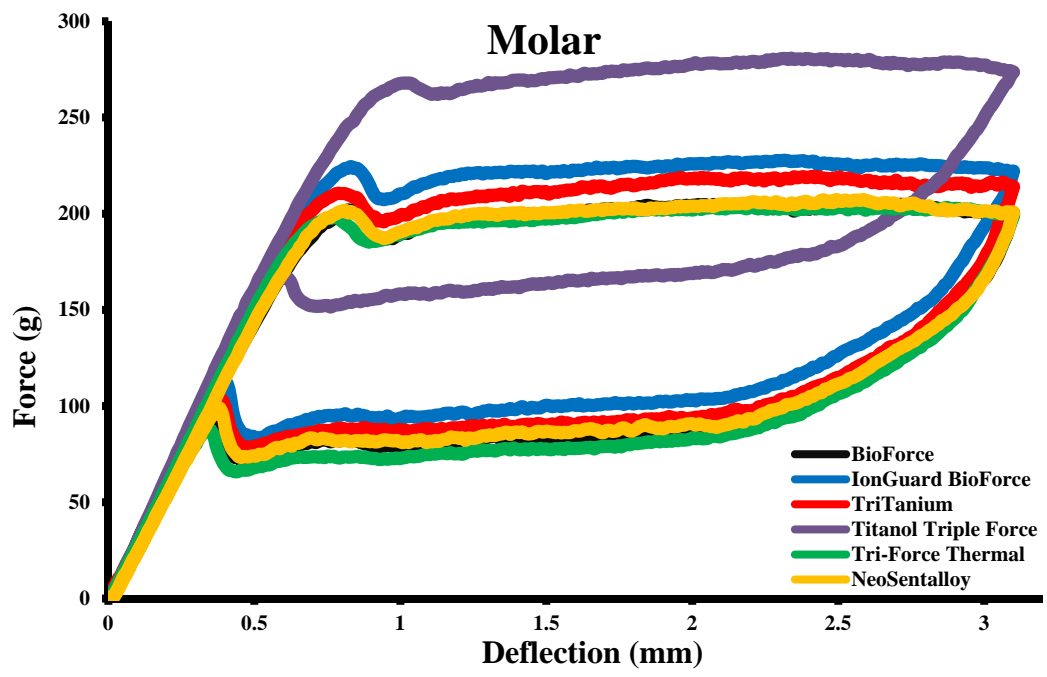


Figure 19. Force deflection curves for Molar segments of six brands of wires

Tables 6-9 display mean stiffness, modulus and loads at deflections of 1 mm, 2 mm and 3 mm during activation and deactivation in the three pointing test for the Anterior, Premolar and Molar segments of the six groups of wire. The activation and deactivation loads show lower values for the anterior and premolar segments when compared with the molar segments. The BioForce archwires showed statistically significant ($p < 0.05$) lower loads during activation and deactivation in the anterior segment when compared with the Control (NeoSentalloy). The IonGuard BioForce and TriTanium wires showed statistically significant ($p < 0.05$) different loads in all three segments when compared with NeoSentalloy with the anterior segment showing lower load deflection values and the premolar and molar segments recording higher loads for the same amount of deflection in the premolar and the molar segments as compared to the NeoSentalloy. Amongst the variable force wires, the Titanol Triple Force wires showed significantly ($p < 0.05$) higher loads amongst all the groups while the Tri-Force thermal wires recorded the lowest values at all three levels of activation and deactivation. However, the force levels for these wires in the premolar and molar segments were in the same range as the NeoSentalloy wires.

Wire Brand	Wire Segment	Activation				
		Stiffness (g/mm)	Modulus (GPa)	Force @ 1 mm (g)	Force @ 2 mm (g)	Force @ 3 mm (g)
BioForce	Anterior	300±6 ^{a,b}	73.9±1.6 ^{a,b}	162±6 ^{b*}	164±6 ^{c*}	155±6 ^{c*}
	Premolar	302±6 ^a	74.5±1.5 ^a	184±4 ^a	192±5 ^b	185±6 ^b
	Molar	296±5 ^b	73.0±1.3 ^b	188±5 ^a	201±6 ^a	199±5 ^a
IonGuard BioForce	Anterior	314±6 ^d	77.3±1.4 ^d	175±4 ^{e*}	178±4 ^{f*}	166±3 ^{f*}
	Premolar	309±8 ^{d,e}	76.2±1.9 ^{d,e}	202±4 ^{d*}	214±6 ^{e*}	208±7 ^e
	Molar	304±8 ^e	75.0±2 ^e	206±8 ^{d*}	222±6 ^{d*}	220±8 ^{i*}
TriTanium	Anterior	312±7 ^g	76.8±1.7 ^g	17±6 ⁱ	180±7 ^{i*}	169±6 ^h
	Premolar	313±7 ^g	77.1±1.8 ^g	200±9 ^h	210±13 ^{h*}	205±17 ^g
	Molar	312±8 ^{g*}	76.8±1.9 ^g	206±9 ^g	222±11 ^{g*}	219±14 [*]
Titanol Triple Force	Anterior	257±27 ^{k*}	63.4±6.7 ^{k*}	212±11 ^{k*}	222±8 ^{k*}	205±7 ^{k*}
	Premolar	311±24 ^j	76.7±5.9 ^j	246±179 ^{j*}	254±16 ^{j*}	247±18 ^{j*}
	Molar	318±18 ^{j*}	78.3±4.4 ^{j*}	252±14 ^{j*}	262±14 ^{j*}	258±17 ^{j*}
Tri-Force Thermal	Anterior	316±11 ^m	78.0±2.7 ^m	166±8 ^{n*}	169±11 ^{n*}	160±12 ^{o*}
	Premolar	317±25 ^{m*}	78.2±6.3 ^{m*}	190±10 ^m	201±13 ^m	196±14 ⁿ
	Molar	315±11 ^{m*}	77.6±2.7 ^{m*}	194±6 ^m	209±7 ^m	207±6 ^m
NeoSentalloy	Anterior	305±5 ^p	75.1±1.2 ^p	186±3 ^q	192±5 ^r	182±9 ^q
	Premolar	302±7 ^p	74.4±1.6 ^p	188±4 ^{p,q}	198±6 ^q	193±8 ^p
	Molar	299±7 ^p	73.7±1.6 ^p	190±3 ^p	203±4 ^p	200±9 ^p

Table 6. Elastic modulus, stiffness and load at 1 mm, 2 mm and 3 mm deflection curves during activation (* represents a significant difference of the other brands from NeoSentalloy; different letters denote significance differences between the segments for a given wire brand)

Wire Brand	Wire Segment	Deactivation				
		Stiffness (g/mm)	Modulus (GPa)	Force @ 3 mm (g)	Force @ 2 mm (g)	Force @ 1 mm (g)
BioForce	Anterior	262±17 ^{b*}	64.6±4.3 ^b	130±5 ^{c*}	52±4 ^{c*}	43±5 ^{c*}
	Premolar	282±8 ^a	69.4±2.1 ^a	158±5 ^b	79±4 ^b	73±4 ^b
	Molar	280±6 ^a	68.9±1.5 ^a	166±5 ^a	85±4 ^a	76±4 ^a
BioForce IonGuard	Anterior	279±8 ^e	68.8±2.1 ^e	143±3 ^{f*}	60±2 ^{f*}	53±2 ^{f*}
	Premolar	286±9 ^d	70.5±2.1 ^d	183±6 ^{e*}	96±4 ^{e*}	90±3 ^{e*}
	Molar	284±9 ^{d,e}	70.0±2.2 ^{d,e}	192±8 ^{d*}	103±8 ^{d*}	95±7 ^{d*}
TriTanium	Anterior	283±11 ^h	69.7±2.7 ^h	144±5 ^{i*}	68±5 ^{i*}	62±6 ^{i*}
	Premolar	292±12 ^g	71.9±3 ^g	175±15 ^{h*}	94±10 ^{h*}	88±10 ^{h*}
	Molar	291±8 ^{g,h}	71.6±1.9 ^{g,h}	187±13 ^{g*}	103±9 ^{g*}	97±9 ^{g*}
Titanol Triple Force	Anterior	244±29 ^{k*}	60.1±7.2 ^{k*}	174±7 ^{k*}	114±9 ^{k*}	106±10 ^{k*}
	Premolar	298±20 ⁱ	73.5±5 ^j	220±15 ^{i*}	143±16 ^{j*}	134±15 ^{j*}
	Molar	304±14 ^{j*}	74.9±3.5 ^{j*}	231±17 ^{j*}	151±14 ^{j*}	140±14 ^{j*}
Tri-Force Thermal	Anterior	259±24 ^{n*}	61.6±12.6 ^{n*}	134±11 ^{o*}	54±11 ^{n*}	45±13 ^{n*}
	Premolar	293±28 ^m	72.1±6.9 ^m	167±13 ⁿ	77±15 ^m	70±15 ^m
	Molar	295±10 ^{m*}	72.8±2.5 ^{m*}	176±7 ^m	86±9 ^m	77±10 ^{m*}
NeoSentalloy	Anterior	280±7 ^p	69.0±1.7 ^p	155±7 ^q	80±3 ^q	77±2 ^q
	Premolar	284±7 ^p	70.0±1.8 ^p	163±7 ^p	83±5 ^q	77±4 ^q
	Molar	283±7 ^p	69.7±1.8 ^p	166±9 ^p	88±4 ^p	81±2 ^p

Table 7. Elastic modulus, stiffness and load at 1 mm, 2 mm and 3 mm deflection curves during deactivation (* represents a significant difference of the other brands from NeoSentalloy; different letters denote significance differences between the segments for a given wire brand)

Wire Segment	Wire Brand	Activation				
		Stiffness (g/mm)	Modulus (GPa)	Force @ 1 mm (g)	Force @ 2 mm (g)	Force @ 3 mm (g)
Anterior	BioForce	300±6 ^B	73.9±1.6 ^B	162±6 ^C	164±6 ^C	155±6 ^C
	IonGuard BioForce	314±6 ^A	77.3±1.4 ^A	175±4 ^B	178±4 ^B	166±3 ^B
	TriTanium	312±7 ^{A,B}	76.8±1.7 ^{A,B}	177±6 ^B	180±7 ^B	169±6 ^B
	Titanol Triple Force	257±27 ^C	63.4±6.7 ^C	212±11 ^A	222±8 ^A	205±7 ^A
	Tri-Force Thermal	316±11 ^A	78.0±2.7 ^A	166±8 ^C	169±11 ^C	160±12 ^C
Premolar	BioForce	302±6 ^G	74.5±1.5 ^G	184±4 ^H	192±5 ^I	185±6 ^I
	IonGuard BioForce	309±8 ^{F,G}	76.2±1.9 ^{F,G}	202±4 ^G	214±6 ^G	208±7 ^G
	TriTanium	313±7 ^{F,G}	77.1±1.8 ^{F,G}	200±9 ^G	210±13 ^G	205±17 ^{G,H}
	Titanol Triple Force	311±24 ^{F,G}	76.7±5.9 ^{F,G}	246±17 ^F	254±16 ^F	247±18 ^F
	Tri-Force Thermal	317±25 ^F	78.2±6.3 ^F	190±10 ^H	201±13 ^H	196±14 ^H
Molar	BioForce	296±5 ^M	73.0±1.3 ^M	188±5 ^M	201±6 ^M	199±5 ^M
	IonGuard BioForce	304±8 ^{L,M}	75.0±2 ^{L,M}	206±8 ^L	222±6 ^L	220±8 ^L
	TriTanium	312±8 ^K	76.8±1.9 ^{K,L}	206±9 ^L	222±11 ^L	219±14 ^L
	Titanol Triple Force	318±18 ^K	78.3±4.4 ^K	252±14 ^K	262±14 ^K	258±17 ^K
	Tri-Force Thermal	315±11 ^K	77.6±2.7 ^K	194±6 ^M	209±7 ^M	207±6 ^M

Table 8. Comparison between Variable Force Wire Brands within different segments during activation (Different letters denote significant differences between the brands for a given segment)

Wire Segment	Wire Brand	Deactivation				
		Stiffness (g/mm)	Modulus (GPa)	Force @ 3 mm (g)	Force @ 2 mm (g)	Force @ 1 mm (g)
Anterior	BioForce	262±17 ^{B,C}	64.6±4.3 ^{A,B}	130±5 ^D	52±4 ^D	43±5 ^C
	IonGuard BioForce	279±8 ^{AB}	68.8±2.1 ^A	143±3 ^C	60±2 ^C	53±2 ^B
	TriTanium	283±11 ^A	69.7±2.7 ^A	144±5 ^B	68±5 ^B	62±6 ^B
	Titanol Triple Force	244±29 ^D	60.1±7.2 ^B	174±7 ^A	114±9 ^A	106±10 ^A
	Tri-Force Thermal	259±24 ^{C,D}	61.6±12.6 ^B	134±11 ^{C,D}	54±11 ^D	45±13 ^C
Premolar	BioForce	282±8 ^G	69.4±2.1 ^G	158±5 ^I	79±4 ^H	73±4 ^H
	IonGuard BioForce	286±9 ^{F,G}	70.5±2.1 ^{F,G}	183±6 ^G	96±4 ^G	90±3 ^G
	TriTanium	292±12 ^{F,G}	71.9±3 ^{F,G}	175±15 ^{G,H}	94±10 ^G	88±10 ^G
	Titanol Triple Force	298±20 ^F	73.5±5 ^F	220±15 ^F	143±16 ^F	134±15 ^F
	Tri-Force Thermal	293±28 ^{F,G}	72.1±6.9 ^{F,G}	167±13 ^{H,I}	77±15 ^H	70±15 ^H
Molar	BioForce	280±6 ^N	68.9±1.5 ^N	166±5 ^N	85±4 ^M	76±4 ^M
	IonGuard BioForce	284±9 ^{M,N}	70.0±2.2 ^{M,N}	192±8 ^L	103±8 ^L	95±7 ^L
	TriTanium	291±8 ^{L,M}	71.6±1.9 ^{L,M}	187±13 ^L	103±9 ^L	97±9 ^L
	Titanol Triple Force	304±14 ^K	74.9±3.5 ^K	231±17 ^K	151±14 ^K	140±14 ^K
	Tri-Force Thermal	295±10 ^{K,L}	72.8±2.5 ^{K,L}	176±7 ^M	86±9 ^M	77±10 ^M

Table 9. Comparison between Variable Force Wire Brands within different segments during deactivation (Different letters denote significant differences between the brands for a given segment)

Figures 20-25 present graphs correlating the A_f temperatures of the Anterior, Premolar and Molar segments of the six archwire groups with the bending forces produced by the wires at 2 mm of deactivation in the three point bending test. The thermally graded wires show a strong correlation between the A_f values of the three segments of the wire and the deactivation at 2 mm, while the Control group does not show a strong correlation, as reflected in the square root of the R^2 value. An inverse linear relation between the A_f temperatures and the deactivation force was observed.

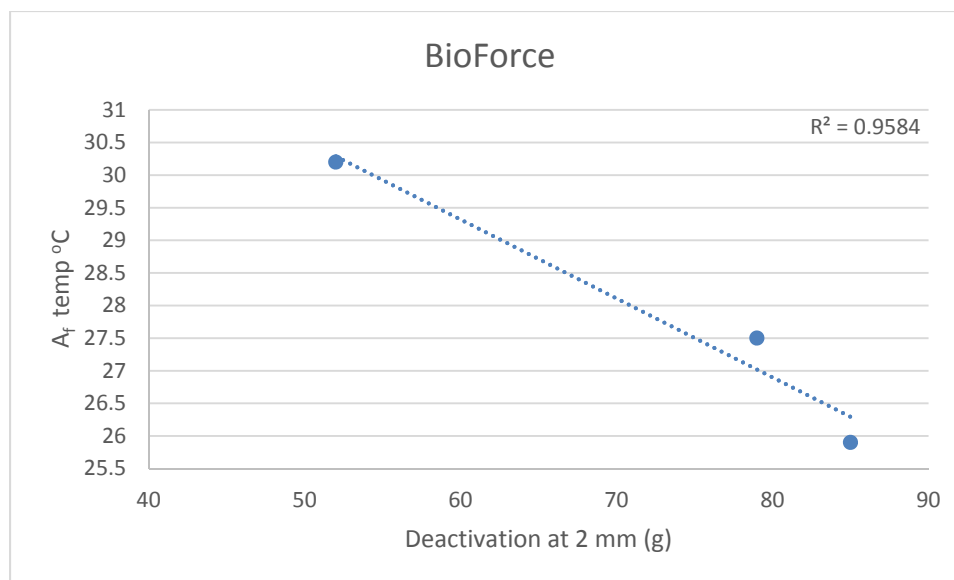


Figure 20. Graph comparing mean A_f temperatures of Anterior, Premolar and Molar segments with deactivation forces at 2 mm for BioForce archwires

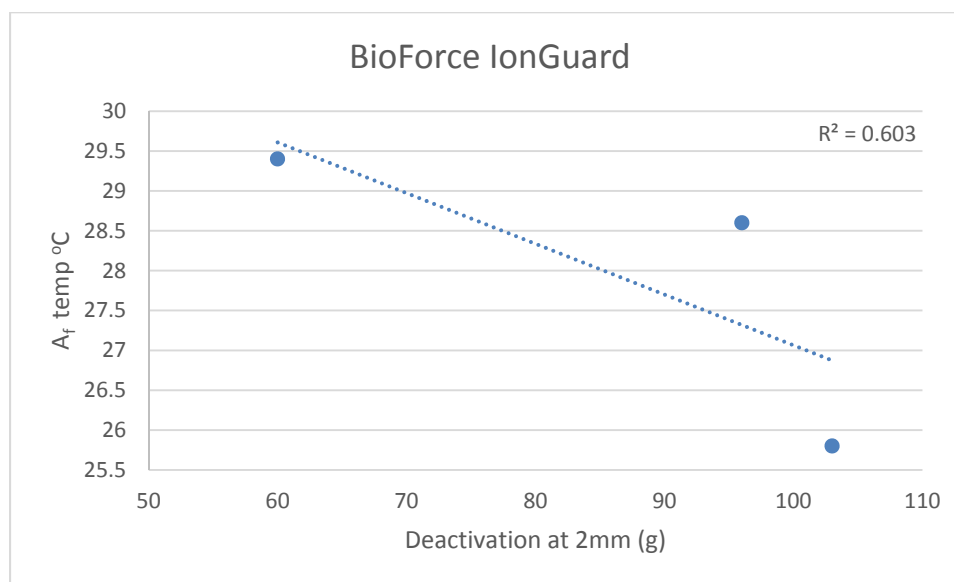


Figure 21. Graph comparing mean A_f temperatures of Anterior, Premolar and Molar segments with bending forces at 2 mm deactivation for BioForce IonGuard archwires

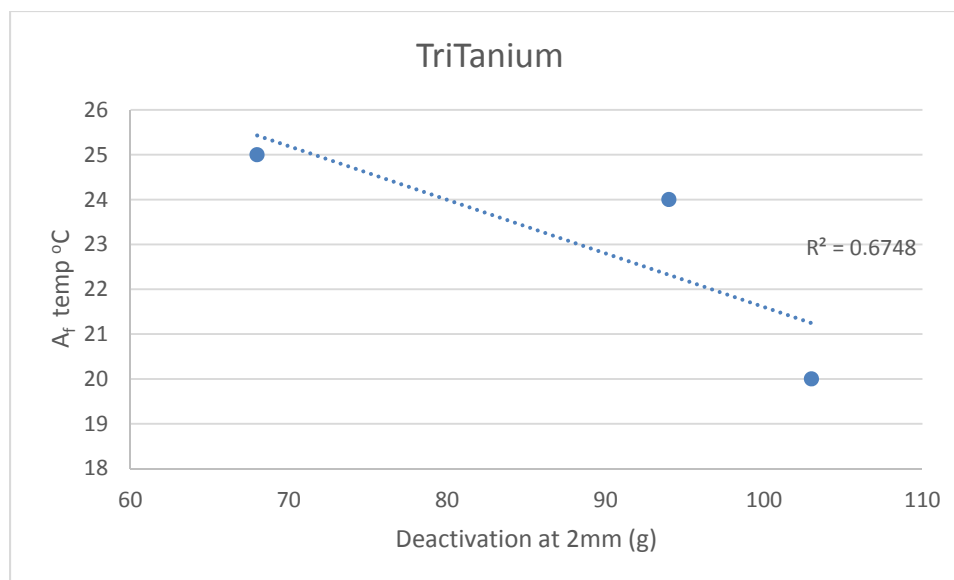


Figure 22. Graph comparing mean A_f temperatures of Anterior, Premolar and Molar segments with deactivation forces at 2 mm for TriTanium archwires

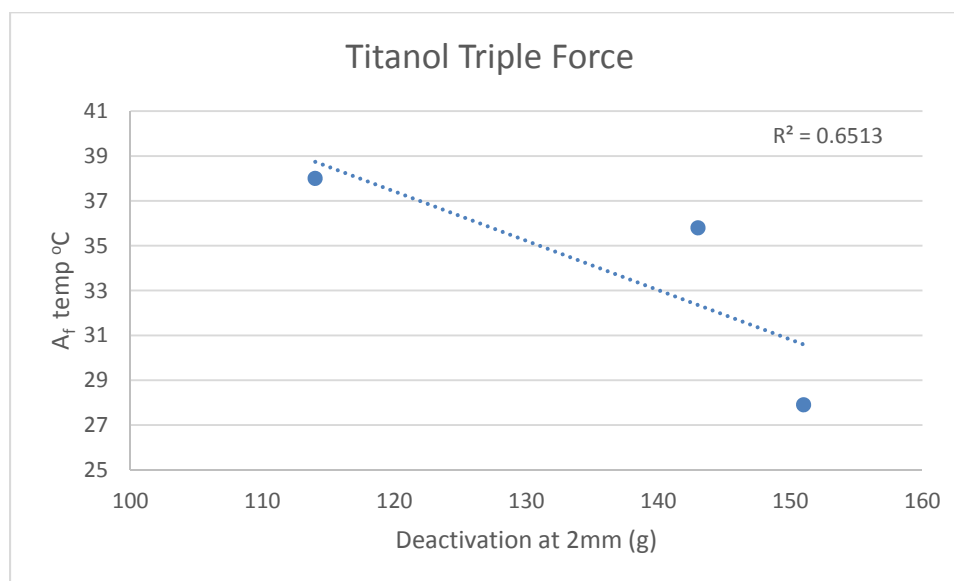


Figure 23. Graph comparing mean A_f temperatures of Anterior, Premolar and Molar segments with deactivation forces at 2 mm for Titanol Triple Force archwires

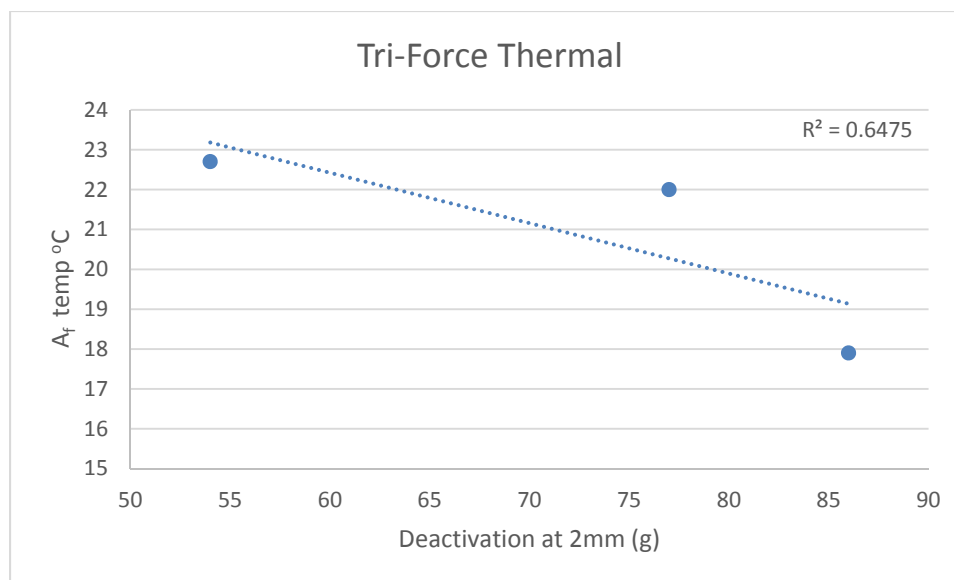


Figure 24. Graph comparing mean A_f temperatures of Anterior, Premolar and Molar segments with deactivation forces at 2 mm for Tri-Force Thermal archwires

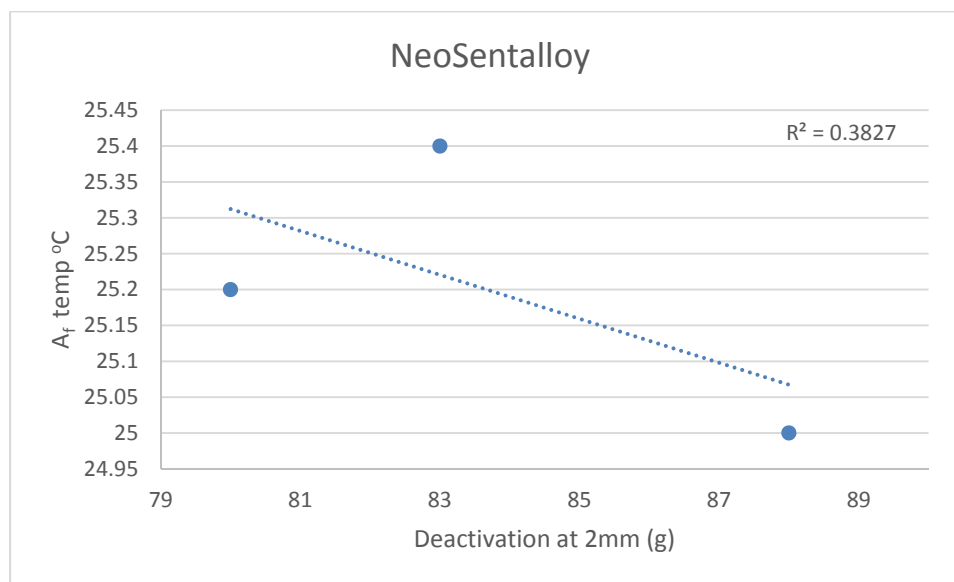


Figure 25. Graph comparing mean A_f temperatures of Anterior, Premolar and Molar segments with deactivation forces at 2 mm for NeoSentalloy archwires

CHAPTER 5

DISCUSSION

Differential Scanning Calorimetric tests showed that when considering all wires and segments, the A_s temperatures ranged from 1.8 to 21.4°C and the A_f temperatures ranged from 17.9 to 38.0°C, indicating the wires were of two types, i.e. superelastic and shape memory wires. Superelastic wires typically have A_f temperatures near or below room temperature, resulting in a wire that is all or nearly all austenite and relegated to the stress-induced phase change. Contrarily, shape memory wires typically have A_f temperatures closer to body/oral temperature, allowing for the austenitic transformation to occur as temperature is raised from room temperature to oral temperature. A comparison of the heating pattern observed for each segment between the variable force archwire brands showed that the Titanol Triple Force wires had the highest transition temperature ranges for all three segments and Tri-Force Thermal had the lowest. Titanol Triple Force wires showed A_f temperatures in the realm of oral cavity temperatures in the anterior and premolar segments, indicating that these wires would be expected to be more thermoresponsive and likely to exhibit shape memory properties when placed in the oral cavity. However, closer inspection of its DSC thermogram and Table 2 shows Titanol Triple Force actually begins transformation from martensite at lower temperatures compared to the other wires. Further, it exhibits a dual peak interpreted as a two-step transformation from martensite to an intermediate R phase or rhombohedral phase and then to austenite. These transformation features complicate the above generalizations and will be discussed below in relation to the bending results.

The heating curves for all but Titanol Triple Force exhibit a single peak upon heating, which is interpreted as a direct martensite to austenite transition. For a few of the brands, notably the BioForce wires and NeoSentalloy, a shoulder on the onset side of the heating peak is noted which would indicate some involvement with the R phase. It is interesting to note that this shoulder is apparent in the molar segments of the BioForce wires but not the anterior. This variation in the recording of the R phase between different nickel-titanium wires has been attributed to the inadequate resolution of traditional DSC in recording small amounts of R phase (Brantley et al., 2003) or to differences in the manufacturing processes of the wires (Biermann et al., 2007). Using temperature-modulated DSC, Brantley et al. (2003) showed that the R phase transition may be present even if not observed with traditional DSC. Given the broadness of the heating peak, one would expect a mixture of phases (austenite, martensite, and possibly R phase if applicable) at room temperature for a majority of the wires/segments. At oral temperature (37°C), also the temperature at which the bending tests were conducted, however, nearly all of the wires will have converted to austenite. The cooling curves of the wires showed the presence of an intermediate R phase which is in harmony with the findings in other studies (Bradley et al., 1996; Brantley & Eliades, 2001).

Quantitative evaluation of the DSC data indicated that the variable force archwires exhibited serially decreasing austenitic finish temperatures from the anterior to premolar and then the molar segments. This decrease in the A_f temperatures was statistically significant between anterior and molar as well as premolar and molar segments of all variable force brands. There was also statistically significant difference between all segments of the BioForce but this trend failed to reach statistical significance

amongst the other brands with differences between most anterior and premolar measured values being insignificant. The Control Group (NeoSentalloy) showed minimal variation in the A_f temperatures between the segments.

The enthalpy changes associated with phase transformations in the wires exhibited a range similar to that observed in superelastic and shape memory wires (Yoneyama et al., 1992; Brantley et al., 2002). However, a comparative evaluation of the enthalpy changes between the different archwire segments did not follow any pattern, indicating that enthalpy served as a poor discriminator of recording transition changes when comparing the behavior of different segments of the variable force archwires.

The three point bending data showed variation in activation stiffness between the three segments of the test wires. However, no evolving trend was observed in the differences in stiffness and elastic moduli in the linear portion of the graphs. This could be because the stiffness was recorded in the initial 0.5 mm deflection of the wire wherein the wire segments were still in their austenitic phase and had not yet begun to show phase transformation superelastic behavior. This initial response of superelastic nickel-titanium wires has been discussed by Santoro et al. (2001). However, the loads at 1 mm, 2 mm and 3 mm activation and deactivation; and the plateau regions in the loading and unloading curves of the load-deflection graphs were lower for the anterior segment as compared to the respective load levels for the premolar and that of the premolar region was lower than for the molar segments. These lower load levels correlate with the A_f temperatures indicating that the stress levels at which the superelastic transformation takes place is lower for the segments of the wire which have higher A_f temperatures. This finding is in consonance with earlier studies (Iijima et al., 2002; Kawashima et al., 1999). The

NeoSentalloy wires showed some significant differences in load levels during activation and deactivation, however the actual difference in deactivation load levels was in the range of about 4-11 gm between the segments as compared to that in the variable force group with much larger differences in actual load levels between the segments.

A comparison of the activation and deactivation loads of the three segments of the five brands of variable force wires with the Control group showed that the anterior segments of BioForce and Tri-Force Thermal archwires showed significantly lower forces for a given amount of deflection as compared to the anterior segment of the Control group which was consistent with their higher A_f temperatures. All three segments of Titanol Triple Force recorded significantly higher force levels than the respective segments of the Control group (NeoSentalloy) as well as amongst the thermally graded wires in spite of their higher A_f temperatures. Variation in composition or cold-working or other proprietary manufacturing processing could be responsible for this behavior, as it has been noted previously that manufacturing processes could alter the thermomechanical behavior of nickel-titanium wires (Pelton et al., 2000). Further, as mentioned above, the Titanol Triple Force wires begin their transformation earlier but undergo a R phase intermediate transition. The R phase has properties closer to austenite than to martensite, which may also explain its increased force values. The BioForce IonGuard wires showed fairly consistent load-deflection values both during activation and deactivation implying that the ion implantation technique used for these wires did not adversely affect their composition and functional performance.

A plot of the A_f temperature versus mean load levels at 2 mm deflection for the three segments of each of the variable force wires showed a strong correlation between

the A_f temperatures and the loads imparted by the different segments of these wires (Figures 20-24). The correlation was negative in that greater A_f temperatures were associated with lower force values. The NeoSentalloy wire, however, showed a poor correlation (Figure 25), as expected because of the little difference in A_f temperature and loads. The unloading characteristics of the wire were compared with the A_f temperatures since these loads are depictive of forces delivered in the clinical situation. When A_f temperature versus mean load levels at 2 mm deflection from all variable force were graphed (not shown), the R^2 value was 0.1291 illustrating that any correlations between A_f temperature and force values are not generalized to all wires but instead to within a given wire with its own characteristics (composition, processing history, etc.).

The three point bending test was used to evaluate the mechanical performance of the wire in a laboratory setting, and the absolute load values obtained through this test cannot be directly extrapolated to the clinical situation since various other factors such as the extent of crowding, anatomic factors such as amount of periodontal bone support, arch length between brackets, dimensions of the wire and friction to name a few contribute to the amount of force delivered by the wire to the teeth. However, a general trend or pattern of behavior of the wires recorded in the test could serve as a predictor of the clinical performance of these wires intraorally. One factor that was noted in this study was that the variable force archwires of different brands exhibited significant variations in the deactivation loads between the brands for the same segments of the wire. Hence, while using these wires, the practitioner should exercise prudent judgement in the use of these wires with due awareness of differences in mechanical characteristics of these wires between the various brands. This difference in behavior between the archwires evaluated

under the conditions of this evaluation could be attributed to differences in proprietary manufacturing processes and composition.

A limitation of the study was that the three sections of the archwires are not as clearly defined by the manufacturers other than the BioForce archwires and hence wire sections were obtained from all the test brands based on the segments defined in the BioForce manufacturer information (Kuftinec, 2008). Also, only the flexural behavior of these wires was tested, and hence variations in superelastic behavior of these wire segments in application of loads under torque between the wire segments were not recorded.

CHAPTER 6

CONCLUSIONS

The following conclusions have been drawn from this study:

1. The Anterior, Premolar and Molar segments showed differences in Austenitic finish temperatures with progressive lowering of these temperatures from the anterior to the premolar and molar segments with significant difference in the anterior and premolar segments and between the premolar and molar segments.
2. The loading and unloading forces of the variable force wires showed differences between the anterior, premolar and molar segments within each brand with lower force levels being recorded by the anterior segments of the wires as compared to the premolar and molar segments.
3. The wires showed a variation in the amount of forces delivered on deflection and the thermal properties for any given segment of the archwire.
4. Little differences were observed between BioForce and IonGuard BioForce indicating the ion bombardment process did not appreciably alter the wire.

REFERENCES

- American Dental Association Council on Scientific Affairs. American National Standard / American Dental Association Specification No. 32 for Orthodontic Wires. ADA Council on Scientific Affairs; 2006
- Airoldi, G., & Riva, G. (1995). Pseudoelasticity of NiTi Orthodontic Wires Modified by Current Methodologies: A Critical Comparison. *J. Phys. IV France*, 05(C2), C2-397-C2-402.
- Andreasen, G., & Barrett, R. (1973). An evaluation of cobalt-substituted nitinol wire in orthodontics. *American Journal of Orthodontics*, 63(5), 462-470.
- Andreasen, G., & Morrow, R. (1978). Laboratory and clinical analyses of nitinol wire. *American Journal of Orthodontics*, 73(2), 142-151.
- Biermann, M., Berzins, D., & Bradley, T. (2007). Thermal Analysis of As-received and Clinically Retrieved Copper-nickel-titanium Orthodontic Archwires. *The Angle Orthodontist*, 77(3), 499-503.
- Bradley, T., Brantley, W., & Culbertson, B. (1996). Differential scanning calorimetry (DSC) analyses of superelastic and nonsuperelastic nickel-titanium orthodontic wires. *American Journal of Orthodontics and Dentofacial Orthopedics*, 109(6), 589-597.
- Braga, L., Vedovello Filho, M., Kuramae, M., Valdrighi, H., Vedovello, S., & Correr, A. (2011). Friction in brackets generated by stainless steel wire, superelastic IonGuard with and without IonGuard. *Dental Press Journal of Orthodontics*, 16(4), 41.e1-41.e6.
- Brantley, W., & Eliades, T. (2001). *Orthodontic materials: Scientific and clinical aspects*. New York: Thieme.
- Brantley, W., Iijima, M., & Grentzer, T. (2003). Temperature-modulated DSC provides new insight about nickel-titanium wire transformations. *American Journal of Orthodontics and Dentofacial Orthopedics*, 124(4), 387-394.
- Burstone, C., Qin, B., & Morton, J. (1985). Chinese NiTi wire: A new orthodontic alloy. *American Journal of Orthodontics*, 87(6), 445-452.
- Gil, F., Cenizo, M., Espinar, E., Rodriguez, A., Ruperez, E., & Manero, J. (2013).). NiTi superelastic orthodontic wires with variable stress obtained by ageing treatments. *Materials Letters*, 104, 5-7.
- Ibe, D., & Segner, D. (1998). Superelastic materials displaying different force levels within one archwire. *Journal of Orofacial Orthopedics / Fortschr Kieferorthop*, 59(1), 29-38.
- Iijima, M., Ohno, H., Kawashima, I., Endo, K., & Mizoguchi, I. (2002). Mechanical behavior at different temperatures and stresses for superelastic nickel-titanium orthodontic wires having different transformation temperatures. *Dental Materials*, 18(1), 88-93.

- Kapila, S., & Sachdeva, R. (1989). Mechanical properties and clinical applications of orthodontic wires. *American Journal of Orthodontics and Dentofacial Orthopedics*, 96(2), 100-109.
- Kawashima, I., Ohno, H., & Sachdeva, R. (1999). Relationship between Af Temperature and Load Changes in Ni-Ti Orthodontic Wire under Different Thermomechanical Conditions. *Dental Materials Journal*, 18(4), 403-412.
- Khier, S., Brantley, W., & Fournelle, R. (1991). Bending properties of superelastic and nonsuperelastic nickel-titanium orthodontic wires. *American Journal of Orthodontics and Dentofacial Orthopedics*, 99(4), 310-318.
- Kuftinec, M. (2008). *GAC White Paper Report. Dentsply*. Retrieved 10 June 2015, from http://www.dentsplygac.eu/sites/all/files/userfiles/France/bioforce_white_paper.pdf
- Kusy, R. (1997). A review of contemporary archwires: their properties and characteristics. *The Angle Orthodontist*, 67, 197-207.
- Miura, F. (1991). *U.S. Patent No. 5,017,133*. Orthodontic Archwire. USA. U.S. Patent and Trademark Office.
- Miura, F., Mogi, M., & Ohura, Y. (1988). Japanese NiTi alloy wire: use of the direct electric resistance heat treatment method. *The European Journal of Orthodontics*, 10(1), 187-191.
- Miura, F., Mogi, M., Ohura, Y., & Hamanaka, H. (1986). The super-elastic property of the Japanese NiTi alloy wire for use in orthodontics. *American Journal of Orthodontics and Dentofacial Orthopedics*, 90(1), 1-10.
- Nikolai, R. (1997). Orthodontic wire: a continuing evolution. *Seminars in Orthodontics*, 3(3), 157-165.
- Pelton, A., DiCello, J., & Miyazaki, S. (2000). Optimization of processing and properties of medical-grade Nitinol wire. In Proceedings of the Int'l Conference on Shape Memory and Superelastic Technologies (SMST-2000) (pp. 361-374). Fremont, California: NDC. Retrieved from <http://www.nitinol.com/media/reference-library/027.pdf>
- Proffit, W., Fields, H., & Sarver, D. (2013). *Contemporary Orthodontics*. St. Louis, Mo.: Elsevier/Mosby.
- Quintao, C., & Brunharo, I. (2009). Orthodontic wires: knowledge ensures clinical optimization. *Dental Press Journal of Orthodontics*, 14(6), 144-157.
- Santoro, M., Nicolay, O., & Cangialosi, T. (2001). Pseudoelasticity and thermoelasticity of nickel-titanium alloys: A clinically oriented review. Part I: Temperature transitional ranges. *American Journal of Orthodontics and Dentofacial Orthopedics*, 119(6), 587-593.
- Santoro, M., Nicolay, O., & Cangialosi, T. (2001). Pseudoelasticity and thermoelasticity of nickel-titanium alloys: A clinically oriented review. Part II: Deactivation forces. *American Journal of Orthodontics and Dentofacial Orthopedics*, 119(6), 594-603.

- Sevilla, P., Martorell, F., Libenson, C., Planell, J., & Gil, F. (2007). Laser welding of NiTi orthodontic archwires for selective force application. *Journal of Material Sciences: Materials in Medicine*, 19(2), 525-529.
- Thompson, S. (2000). An overview of nickel-titanium alloys used in dentistry. *International Endodontic Journal*, 33(4), 297-310.
- Yoneyama, T., Doi, H., Hamanaka, H., Yamamoto, M., & Kuroda, T. (1993). Bending properties and transformation temperatures of heat treated Ni-Ti alloy wire for orthodontic appliances. *Journal of Biomedical Materials Research*, 27(3), 399-402.
- Yoneyama, T., Doi, H., Hamanaka, H., Okamoto, Y., Mogi, M., & Miura, F. (1992). Super-Elasticity and Thermal Behavior of Ni-Ti Alloy Orthodontic Arch Wires. *Dental Materials Journal*, 11(1), 1-10,111.
- Wichelhaus, A., Geserick, M., Hibst, R., & Sander, F. G. (2005). The effect of surface treatment and clinical use on friction in NiTi orthodontic wires. *Dental Materials*, 21(10), 938-945.